

## Review

## Magma chambers: Formation, local stresses, excess pressures, and compartments

Agust Gudmundsson

Department of Earth Sciences, Royal Holloway University of London, Egham TW20 0EX, UK

## ARTICLE INFO

## Article history:

Received 7 January 2012

Accepted 20 May 2012

Available online 1 June 2012

## Keywords:

Magma chambers

Crustal stresses

Stress concentrations

Dykes

Sills

Volcanic eruptions

## ABSTRACT

An existing magma chamber is normally a necessary condition for the generation of a large volcanic edifice. Most magma chambers form through repeated magma injections, commonly sills, and gradually expand and change their shapes. Highly irregular magma-chamber shapes are thermo-mechanically unstable; common long-term equilibrium shapes are comparatively smooth and approximate those of ellipsoids of revolution. Some chambers, particularly small and sill-like, may be totally molten. Most chambers, however, are only partially molten, the main part of the chamber being crystal mush, a porous material. During an eruption, magma is drawn from the crystal mush towards a molten zone beneath the lower end of the feeder dyke. Magma transport to the feeder dyke, however, depends on the chamber's internal structure; in particular on whether the chamber contains pressure compartments that are, to a degree, isolated from other compartments. It is only during large drops in the hydraulic potential beneath the feeder dyke that other compartments become likely to supply magma to the erupting compartment, thereby contributing to its excess pressure (the pressure needed to rupture a magma chamber) and the duration of the eruption.

Simple analytical models suggest that during a typical eruption, the excess-pressure in the chamber decreases exponentially. This result applies to a magma chamber that (a) is homogeneous and totally fluid (contains no compartments), (b) is not subject to significant replenishment (inflow of new magma into the chamber) during the eruption, and (c) contains magma where exsolution of gas has no significant effect on the excess pressure. For a chamber consisting of pressure compartments, the exponential excess-pressure decline applies primarily to a single erupting compartment. When more than one compartment contributes magma to the eruption, the excess pressure may decline much more slowly and irregularly.

Excess pressure is normally similar to the in-situ tensile strength of the host rock, 0.5–9 MPa. These in-situ strength estimates are based on hydraulic fracture measurements in drill-holes worldwide down to crustal depths of about 9 km. These measurements do not support some recent magma-chamber stress models that predict (a) extra gravity-related wall-parallel stresses at the boundaries of magma chambers and (b) magma-chamber excess pressures prior to rupture of as much as hundreds of mega-pascals, particularly at great depths.

General stress models of magma chambers are of two main types: analytical and numerical. Earlier analytical models were based on a nucleus-of-strain source (a 'point pressure source') for the magma chamber, and have been very useful for rough estimates of magma-chamber depths from surface deformation during unrest periods. More recent models assume the magma chamber to be axisymmetric ellipsoids or, in two-dimensions, ellipses of various shapes. Nearly all these models use the excess pressure in the chamber as the only loading (since lithostatic stress effects are then automatically taken into account), assume the chamber to be totally molten, and predict similar local stress fields. The predicted stress fields are generally in agreement with the world-wide stress measurements in drill-holes and, in particular, with the in-situ tensile-strength estimates.

Recent numerical models consider magma-chambers of various (ideal) shapes and sizes in relation to their depths below the Earth's surface. They also take into account crustal heterogeneities and anisotropies; in particular the effects of a nearby free surface and horizontal and inclined (dipping) mechanical layering. The results show that the free surface may have strong effects on the local stresses if the chamber is comparatively close to the surface. The mechanical layering, however, may have even stronger effects. For realistic layering, and other heterogeneities, the numerical models predict complex local stresses around magma chambers, with implications for dyke paths, dyke arrest, and ring-fault formation.

© 2012 Elsevier B.V. All rights reserved.

## Contents

1. Introduction . . . . .	20
2. Definition of a magma chamber . . . . .	21
3. Formation and geometry of magma chambers . . . . .	21
4. Crustal stresses . . . . .	27
5. Stresses and pressures associated with dykes and sills . . . . .	28
6. Stresses around magma chambers . . . . .	32
6.1. Stresses at magma-chamber initiation . . . . .	32
6.2. Different approach to magma-chamber stress modelling . . . . .	33
6.2.1. The first point . . . . .	33
6.2.2. The second point . . . . .	34
6.2.3. The third point . . . . .	34
7. Chamber pressure variation during an eruption: effects of compartments . . . . .	34
8. Discussion . . . . .	37
9. Conclusions . . . . .	38
Acknowledgements . . . . .	39
References . . . . .	39

## 1. Introduction

A magma chamber is the heart of every active major polygenetic volcano (Fig. 1). Thus, each major volcanic structure, such as a stratovolcano, a collapse caldera, or a large shield volcano (a basaltic edifice), is supplied with magma from a (comparatively shallow) crustal magma chamber. Formation of a major volcanic edifice is the consequence of the existence of a magma chamber—not the other way around. The chamber acts as a collector of magma from the deeper source (here referred to as a reservoir) and channels that magma to a limited area at the surface above where the volcano builds up. If there were no shallow magma chambers, the volcanic activity would be much more evenly distributed than it actually is, both

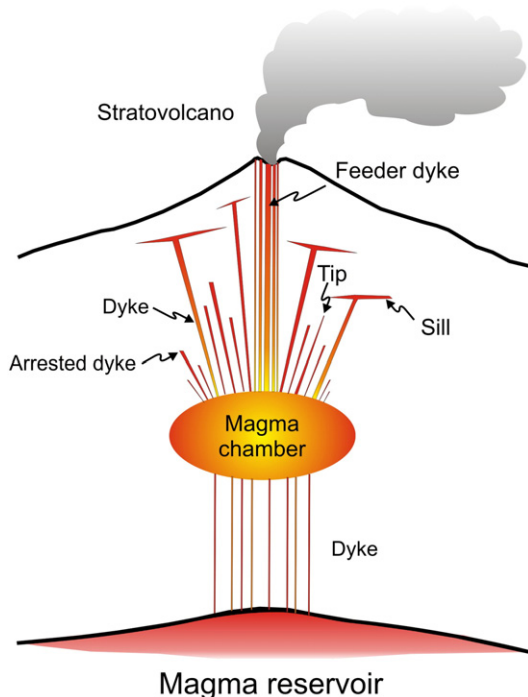


**Fig. 1.** Schematic illustration of a volcanic edifice, here a stratovolcano. The magma chamber acts as a sink for magma from a deeper magma accumulation zone (here referred to as a reservoir) and a source for inclined sheets, sills, and dykes (including feeder dykes). Many of the dykes become arrested, some becoming deflected into sills. The volcano builds up into a cone because the chamber channels magma to a limited area on the surface.

as regards volume and particularly as regards frequency, along active volcanic zones and fields.

In order to understand volcano behaviour, in particular the size-distributions, the volumetric flow rates, and the duration of its eruptions, it is necessary to have a reliable knowledge of the mechanical behaviour of the associated magma chamber. That knowledge should include the following points:

- (1) How the host rock and the matrix of the chamber itself respond to stress and fluid pressure changes;
- (2) What the material properties of the chamber and its host rock are and how these may change with time;
- (3) How the shape and loading of the chamber affects the local stress fields inside and outside the chamber;
- (4) The likelihood of rupture with a dyke, sheet, or sill injection and, eventually, eruption.

For an eruption to occur, the necessary condition is that the magma chamber or reservoir ruptures and a fluid-driven fracture (usually a dyke or an inclined sheet) is able to propagate from the chamber to the surface. In some volcanoes, such as Stromboli (Italy) and Sakura-Jima (Japan), as well as in some active lava lakes, such as in Kilauea (Hawaii), Nyiragongo and Erta Ale (Africa), and Mount Erebus (Antarctica), there is quasi-continuous eruptive activity over long periods of time (Simkin and Siebert, 2000; Frank, 2003; Rosi et al., 2003; Siebert et al., 2010). In these cases, the conduit may be continuously open. However, volcanoes with these types of eruptions are rare in comparison with those where a new fluid-driven fracture forms during each eruption. Also, it is likely that even if some of the quasi-continuous eruptions may last for tens, hundreds or (in case of Stromboli) perhaps a couple of thousand years (Kilburn and McGuire, 2001; Rosi et al., 2003; Siebert et al., 2010), the continuous eruptions are short-lived in comparison with the overall lifetime of the volcano itself—of the order of  $10^5$  to  $10^6$  years. Thus, for most of the time, in most volcanoes, and for most eruptions, a magma-chamber rupture and fluid-driven fracture propagation to the surface is the mechanism of eruption.

Both the magma-chamber rupture and the fluid-driven fracture propagation to the surface depend primarily on the local stresses inside the volcano and around the magma chamber. This has been widely recognised in the past decades, with many papers and books focusing on modelling the stress and displacement fields in volcanoes. These models fall broadly into two basic groups. First, those that attempt primarily to explain the surface deformation and the depth to the associated magma chamber during unrest periods. Second, those that attempt to model the stress fields around the

magma chamber and inside the volcano itself in relation to the conditions for rupture and dyke/sheet propagation to the surface.

In the first group, where the main aim is to understand surface deformation during unrest periods and eruptions, the best known is the 'Mogi model' (Mogi, 1958). This model, initially derived from nucleus-of-strain solutions in solid mechanics (Melan, 1932; Mindlin, 1936) and applied to volcanoes by Anderson (1936), focuses on explaining volcano surface deformation during an unrest period in terms of the depth and pressure of a magma chamber (modelled as a nucleus of strain, that is, a point pressure source). Since the magma chamber is regarded as the product of the source radius and the excess pressure, the excess pressure and the size of the chamber cannot be estimated independently. There is thus no information provided as to the stresses that control magma-chamber rupture, namely the stresses that concentrate around the magma chamber itself. The 'Mogi model' and its application to surface deformation, including caldera formation, is discussed in detail by Mogi (1958), Dzurisin (2006), Kusumoto and Takemura (2005), Gudmundsson (2006), Sturkell et al. (2006), Poland et al. (2006), Kusumoto and Gudmundsson (2009), and Segall (2010).

Extensions of the 'Mogi model' include those of Davis (1986) where the chamber is no longer assumed spherical (a point source) but rather an arbitrary oriented triaxial ellipsoidal cavity. As a rule, however, the nucleus-of-strain models regard the crustal segment hosting the magma chamber as a homogeneous, isotropic, elastic half-space, thereby ignoring all mechanical layering and heterogeneities of the segment. Masterlark (2007) found significant differences between depth estimates for magma chambers based on homogeneous and isotropic elastic half spaces and those based on layered crustal segments. Also, numerical models indicate that the surface stress and deformation above magma chambers and dykes, for example, depend strongly on the mechanical layering of the crustal segments hosting these structures (Gudmundsson, 2011a). Using numerical and analytical methods, recent models consider the effects of heterogeneous, layered, and anelastic crustal segments to infer magma-chamber shape and inflation mechanisms (e.g., Bonafede et al., 1986; Bonaccorso et al., 2005; Trasatti et al., 2005; Bonafede and Ferrari, 2009; Trasatti et al., 2011).

In the second group, the main aim of modelling is to understand the stress (and displacement) fields inside the volcano and how they affect magma-chamber rupture, dyke/sheet propagation, and the likelihood of eruption during an unrest period. These models are also used to explain the surface deformation, not only in terms of magma-chamber inflation and deflation, but also as regards the stress and deformation induced at the surface by upward-propagating dykes. This second group of models has received increasing attention in the past few decades. However, while there is general agreement as to some aspects of the modelling, such as the common magma-chamber shapes, there are divergent views as to the theoretical stresses around magma chambers and how to model them.

As suggested in the invitation to write this paper, one of its principal aims is to discuss these divergent views and to clarify how the state of stress around a magma chamber should be calculated and compared with in-situ measurements of stresses and strengths in drill-holes worldwide. Since the stress field inside a volcano, and in particular around its magma chamber, largely controls the volcano deformation and the likelihood and duration of its eruptions, it is of fundamental importance that there should be a clear theory as to how to calculate the local stress field around a magma chamber. The local stress field around a chamber and inside the associated volcano, however, depend much on the shape and size of the chamber which, in turn, are related to the initiation and evolution of the chamber. A second aim of this paper is thus to review various likely scenarios for the initiation and geometric development of magma chambers. The local stresses inside a volcano determine not only the condition for magma-chamber rupture and dyke propagation to the surface, but also affect the behaviour, in particular the volumetric flow rate

and the duration, of the eruption. The third aim of the paper is to provide simple analytical results on excess-pressure variation in a chamber during eruption. In detail, the excess-pressure (and compositional) variation during an eruption depend on whether the chamber contains pressure compartments, as are well known from many hydrocarbon reservoirs. Compartments depend on the local stresses, pressures, and mechanical properties of the chamber. The fourth and final aim is thus to touch briefly on the topic of magma-chamber compartments. The paper provides a review and analysis of many existing ideas and models, but presents also some new ideas, particularly as regards excess-pressure variations and compartments in magma chambers.

## 2. Definition of a magma chamber

A magma chamber is a partially or totally molten body located in the crust and supplied with magma from a deeper source, a reservoir (Fig. 1). While active, a magma chamber acts as a sink for magma from the deeper reservoir, and as a source for magma injections (dykes, sheets, sills) into the surrounding crust and the associated volcano. Some magma chambers, particularly small sill-like chambers during their early stages of development, may be totally molten. Other chambers, however, are partially molten from their initiation, or become so quickly during their evolution. A large part of the chamber may then consist of a crystal mush, a matrix, which behaves as poroelastic (Maaloe and Scheie, 1982; McKenzie, 1984; Gudmundsson, 1987; Marsh, 1989, 2000; Sinton and Detrick, 1992). Under these conditions, only the central or upper part of the chamber may be totally molten and the lower, and greater, part a hot, partially molten crystalline mush or matrix. This latter appears to be common for the magma chambers at mid-ocean ridges (Macdonald, 1982; Sinton and Detrick, 1992; Mutter et al., 1995; MacLeod and Yaouancq, 2000; Singh et al., 2006; Canales et al., 2009).

An active (fluid) magma chamber has clearly mechanical properties that differ from those of the host rock. But even a solidified magma chamber, a pluton, with the same chemical composition as the host rock (which is rare) may differ mechanically from the host rock. This applies particularly when the pluton has a higher temperature than the host rock and follows because the mechanical properties of rocks change with temperature. In particular, Young's modulus (stiffness) depends on temperature (Balme et al., 2004). When the chamber is totally molten, it acts as a fluid-filled cavity, and when it is partially molten or, alternatively, solidified but still hot, as a comparatively compliant (soft) inclusion (Andrew and Gudmundsson, 2008; Gudmundsson, 2011a). When the solidified chamber rock has reached the same temperature as the host rock, the chamber is referred to as a pluton. Most plutons are of rock types that differ mechanically from those of the host rocks: for example, the pluton may be a gabbro body located in a (mostly) basaltic lava pile (Fig. 2). The pluton (the fossil magma chamber) then acts as a stiff inclusion. All cavities and inclusions modify the local stress field and concentrate stresses. However, the induced stresses depend much on the geometry of the cavity/inclusion (Savin, 1961; Boreis and Sidebottom, 1985; Tan, 1994; Saada, 2009). This is one reason why knowing the shape of a magma chamber, active or fossil, is of great importance for understanding the local stress field around the chamber.

## 3. Formation and geometry of magma chambers

Most crustal magma chambers presumably develop from sills (Pollard and Johnson, 1973; Gudmundsson, 1990; Annen and Sparks, 2002; Kavanagh et al., 2006; Menand, 2008; Menand et al., 2010; Menand, 2011; Menand et al., 2011). In fact, many chambers, particularly at mid-ocean ridges, maintain the sill-like geometry of at least the molten part throughout their lifetimes (Macdonald, 1982; Sinton

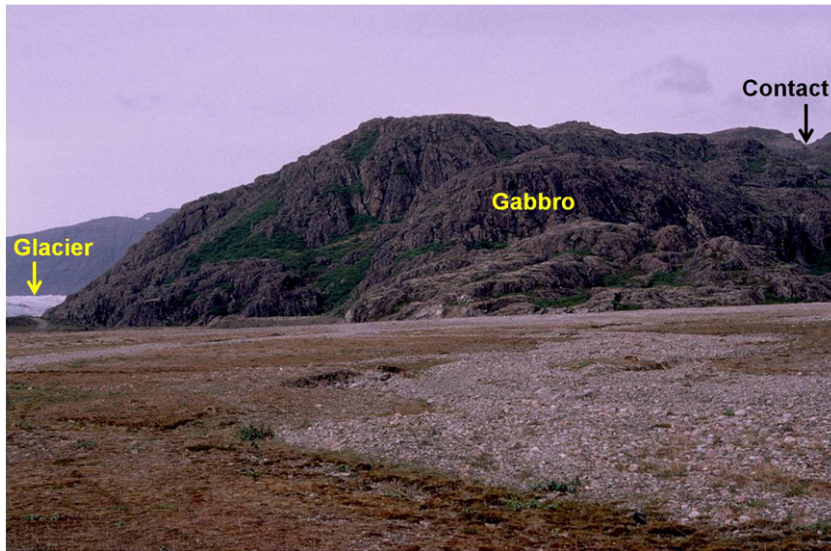


**Fig. 2.** Part of a fossil magma chamber in Geitafell, Southeast Iceland. View north, the exposed part of the chamber, a gabbro pluton, is at a depth of about 2 km below the initial top of the associated volcano and is located within a pile of (mostly) basaltic lava flows with mechanical properties that differ from those of the pluton. At the east (right) contact (marked) of the pluton, there is an abrupt change from gabbro to close to 100% inclined sheets and dykes (cf. Gudmundsson, 2011b, Fig. 3). The width (lateral dimension) of the part of the gabbro pluton exposed here is about 400 m and the height of the cliffs as see here is about 80 m.

and Detrick, 1992; Mutter et al., 1995; MacLeod and Yaouancq, 2000; Singh et al., 2006; Canales et al., 2009). Most sills, however, do not develop into magma chambers. Thus, special conditions must be met for a sill to evolve into a magma chamber. These include that the initial sill must (1) be comparatively thick, normally at least tens of metres (but depends on the spreading rate) and (2) receive magma so frequently (through dykes) that it stays liquid for a considerable time and has the chance to grow into a chamber (Gudmundsson, 1990; Menand et al., 2010, 2011). The formation of sills, that is, the conditions for dykes deflecting into sills, is discussed by Pollard and Johnson (1973), Menand (2008), Gudmundsson (2011b), Menand et al. (2010, 2011), and Maccaferri et al. (2011).

If most magma chambers initiate from sills, then it follows that the initial chamber shape is sill-like. Sills, however, have many different shapes (Fig. 3). Perhaps the most common sill shapes are straight

(Fig. 3a,c), concave-upwards bending (Fig. 3b), and stair-case (Fig. 3d), of which the saucer-shape is a special case. Many magma chambers that have been detected beneath mid-ocean ridges appear comparatively straight, as inferred from seismic studies. Such seismic studies, however, have generally a low resolution and do not allow us to decide on the detailed shapes.

Calculations show that the chances of a sill developing into a magma chamber in an area undergoing extension (such as at a divergent plate boundary) depend largely on a combination of spreading rates and cooling rates (Gudmundsson, 1990). This follows because the rate of injection of dykes that could meet the sill and supply magma to it is directly proportional to the associated spreading rate. The higher the dyke-injection rate, the greater the chances of a dyke meeting the sill, and thus the greater the probability of that sill developing into a magma chamber. This conclusion is supported

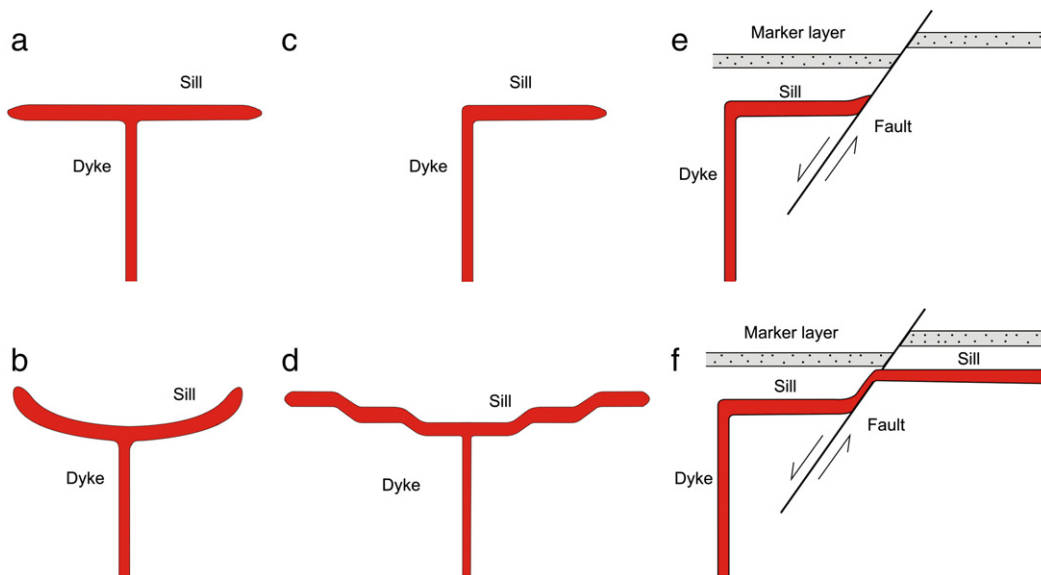


**Fig. 3.** Various stress and mechanical conditions favour the deflection of dykes into sills (cf. Kavanagh et al., 2006; Gudmundsson, 2011b; Menand, 2011; Menand et al., 2011). The resulting sills can have various forms, some of which are shown here. (a) Double-deflected straight sill. (b) Concave or upward-bending sill. (c) Single-deflected straight sill. (d) Stair-case-shaped double-deflected sill, a subgroup of which is the saucer-shaped (disc-shaped) sill. (e) A single-deflected sill arrested by a fault. (f) A single-deflected sill that propagates towards and up along the fault; the sill follows the fault for a while and then propagates parallel with a contact in the footwall.

by there being many more, and more extensive, shallow magma chambers at fast-spreading ridges than at slow-spreading ridges (Macdonald, 1982; Sinton and Detrick, 1992; Mutter et al., 1995; MacLeod and Yaouancq, 2000; Singh et al., 2006; Canales et al., 2009).

In mafic (basic) fossil magma chambers, the contacts between individual sills injected during the formation of the magma chamber cannot normally be identified. This is because the low-viscosity basaltic magma supplied through a new sill injection normally becomes mixed with the existing magma in the earlier sills. When multiple basaltic sills are seen and clearly identified as such in the field (Fig. 4), it is because they formed over a time period too long for the successive sill injections to develop into a single magma body, a chamber.

By contrast, in some felsic (acid) fossil magma chambers formed by sill injections, and presently exposed as plutons, the individual sills can

be identified. This is primarily because of the more highly viscous magma of the sills makes mixing of the new and old magma, if both are acid, less likely than in the case of basaltic sills. One particularly clear example of a fossil acid magma chamber formed by sill injections occurs in Slaufudalur in East Iceland (Fig. 5; Gudmundsson, 2011b). Here the contacts between the sills are clearly seen since they form distinct layers. The layers dip 5–10°NW, similar to that of the lava flows that form the host rock of the pluton, and their thicknesses are mostly 15–50 m (Fig. 5; Beswick, 1965). This magma chamber formed by the piling up of 15–50 m thick acid (granophytic) sills. With an exposed maximum thickness of about 700 m, it clearly formed through many sill injections. There are many other examples of felsic magma chamber/pluton formation through numerous, commonly sill-like, injections. For example, many large granitic plutons are now thought to have

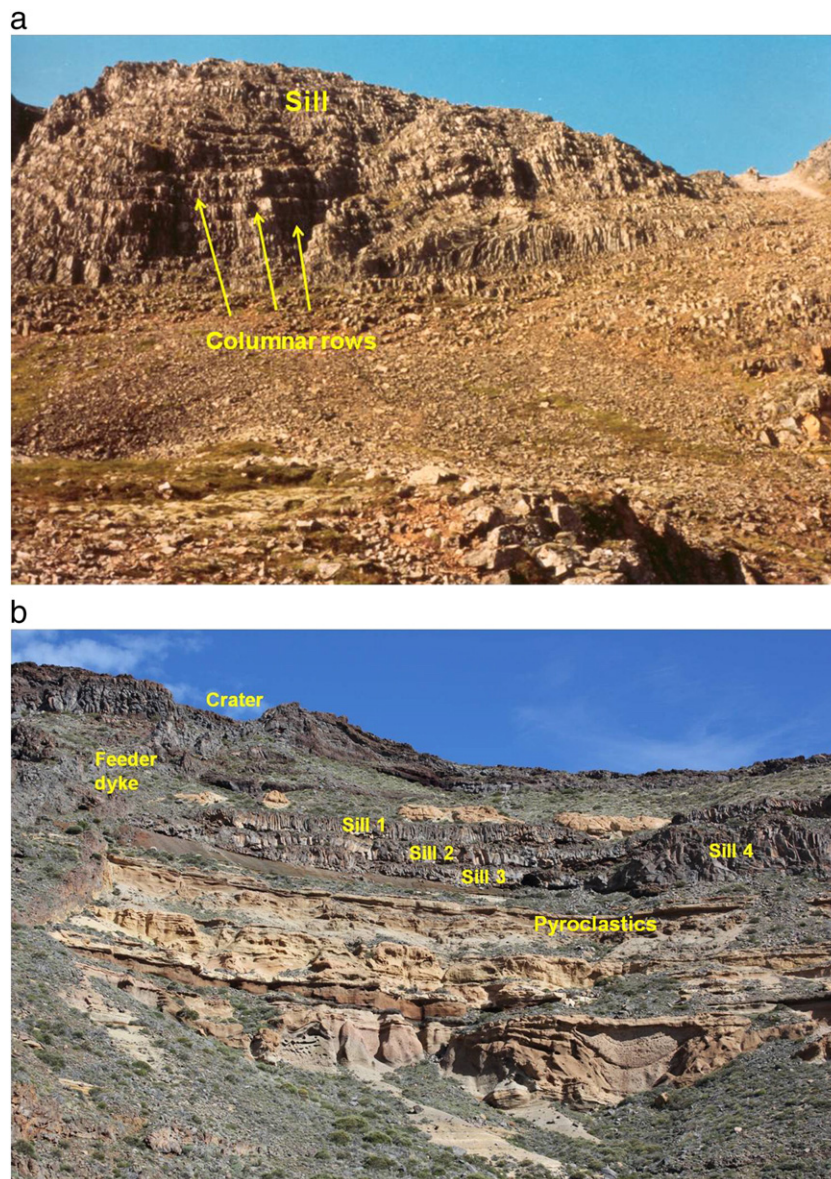


**Fig. 4.** (a) Part of a thick basaltic sill in East Iceland. The sill is 120-m thick, composed of at least 16 columnar rows (some indicated) and thus a multiple intrusion. The overall shape of the sill is concave (Fig. 3b), as is seen from a greater distance (Gudmundsson, 2011b, Fig. 12), and is located at a depth of about 800 m below the top of the rift zone at the time of sill emplacement. The exposed lateral dimension of the sill is about 3 km, but the rest is eroded away so that its initial dimension is unknown. The sill did not develop into a magma chamber, presumably because the rate of dyke injections was so low that individual columnar rows became solidified before the subsequent ones were injected (cf. Fig. 8). (b) View east, a cluster or complex of sills in the caldera walls of Las Canadas in Tenerife (Canary Islands). This cluster formed at about 100 m below the free surface of the volcano; a crater is seen at the surface (and its feeder dyke is indicated; see Fig. 13 for the details of the feeder). The sill cluster (marked by Sill 1, Sill 2, Sill 3 and Sill 4) extends laterally for many hundred metres (only a part of the complex is seen here) and reaches thicknesses of tens of metres. Here, however, the total thickness of the cluster is about 20 m. The sills formed at contacts between mechanically dissimilar pyroclastic rocks (light-brown to dark-brown in colour; one layer indicated) and elsewhere in the wall at contacts between stiff lava flows and pyroclastic rocks.

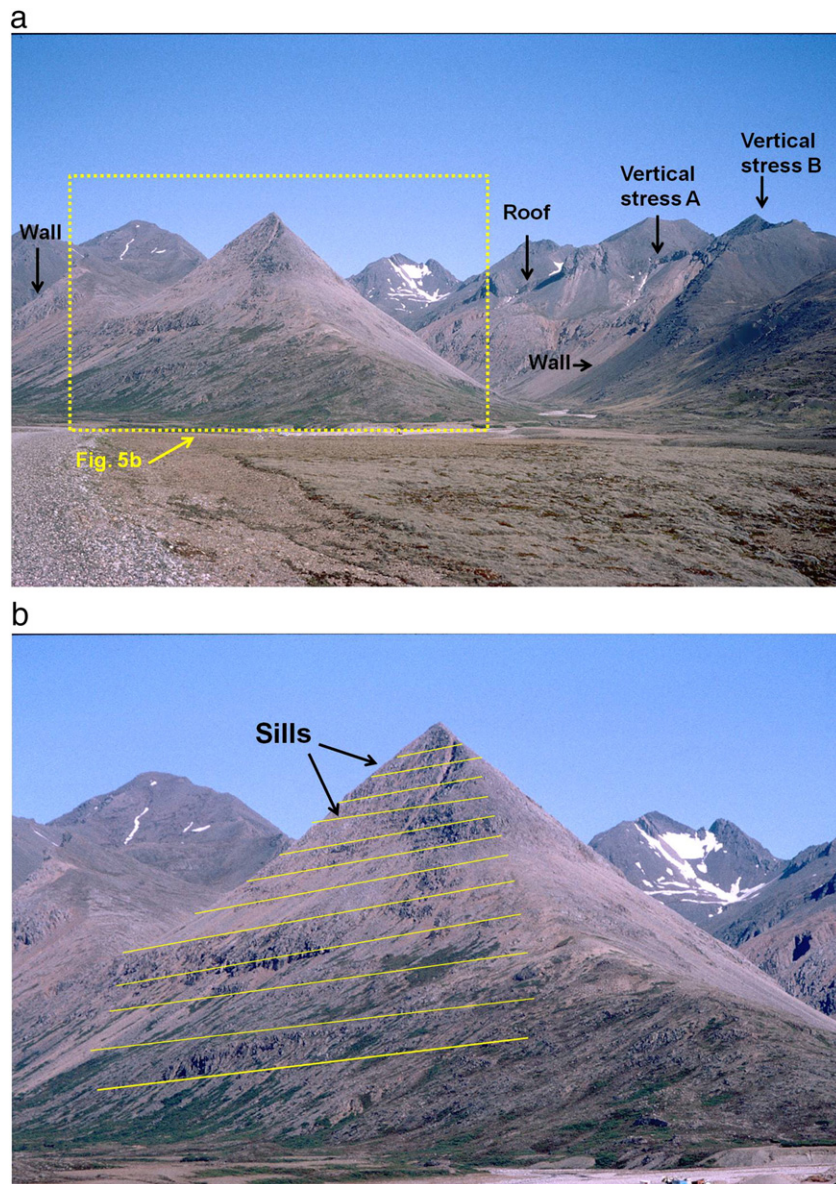


**Fig. 5.** Part of the fossil magma chamber at Slaufudalur, Southeast Iceland (located in Gudmundsson, 2011b, Figs. 4, 14). (a) View northwest, the present pluton is composed of granophyre and has an exposed volume of about  $10 \text{ km}^3$ . Many of the walls are well exposed—two are indicated here. Part of the roof is also exposed, through which many felsic dykes have been injected. Many of these dykes presumably became arrested, that is, were non-feeders, which is one major reason why their contacts with the magma chamber remained filled with magma (did not close, as they normally would tend to do at the end of an associated eruption). The vertical stress at points A and B refers to the discussion about ‘wall-parallel’ stresses in Section 6. Fig. 5b. (b) The Slaufudalur magma chamber was generated through injection of numerous granophyre sills. Some of the sills can be seen as crude layering, most of the layers (sills) being 15–50 m thick (Beswick, 1965; cf. Gudmundsson, 2011b).

formed through many dyke-fed injections of sills or sheets, generating an overall flat-lying (sill like) magma body (Petford et al., 2000).

The mode of emplacement of the Slaufudalur sills, as for most sills, was forceful, that is, the host rock became deformed. This is easily seen because of change in the dip of the host rock close to the pluton. In the basaltic lava pile west of Slaufudalur (not seen in Fig. 5) the lavas are not disturbed by the pluton and the regional dip is  $8\text{--}10^\circ\text{NW}$ , and thus towards the pluton. But close to the pluton, at the entrance of the valley of Slaufudalur (Fig. 5) the dip of the lava flows is  $11^\circ\text{E}$ , that is, away from the pluton. It follows that the lava pile has been tilted by  $15\text{--}20^\circ$  during the emplacement of the Slaufudalur magma chamber. The dykes and inclined sheets that dissect the roof of the pluton (Fig. 5) demonstrate that it functioned as a magma chamber, that is, sent off dykes. Presumably, some of the injected dykes supplied magma to a volcano at the surface.

Most sills and laccoliths and other potential magma-chamber intrusions show clear evidence of being forceful intrusions (Fig. 6). This

means that the space for the intrusion is generated by the fluid-overpressure driven opening displacement of the fracture walls. Laccoliths, in particular, show clear evidence of bending and fracturing of the roof layers (Fig. 6; Hawkes and Hawkes, 1933; Pollard and Johnson, 1973; Pasquare and Tibaldi, 2007). The roofs of sills emplaced in sedimentary rocks also commonly show evidence of forceful emplacement (Hansen and Cartwright, 2006). A large fraction of the space needed for the sills and other magma-chamber intrusions is thus generated by forceful uplift or up-bending of the roof, as well as down-bending of the floor. There are other factors that may significantly affect the exact emplacement mechanics, in particular whether up-bending (as in laccoliths) or down-bending (as presumably in many sill-like intrusions) dominates (Petraske et al., 1978). These include the mechanical layering of the host rock, the depth of emplacement, and the size of the sill-like intrusion.

The geometric evolution of the magma chamber after the initial sill emplacement varies considerably and depends on many factors

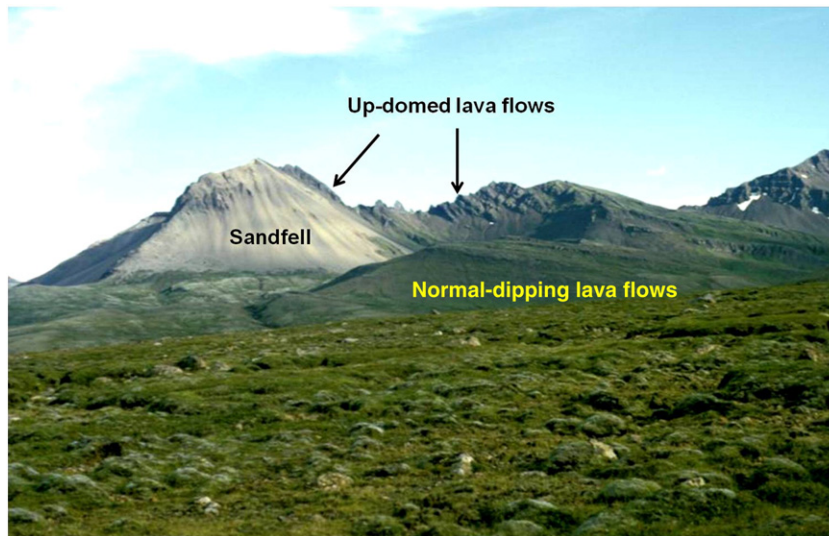


**Fig. 6.** Sandfell, a felsic laccolith in East Iceland. Like most plutons in Iceland, Sandfell shows clear evidence of being a forceful intrusion; in this case, up-doming or tilting of the lava flows close to and on the top of the laccolith. The local dips of the lava flows reach 34–36°, whereas the regional dip of the lava flows (the ‘normal-dipping lava flows’), away from the laccolith, is about 8°. The top of the mountain is at 743 m a.s.l., and the thickness of the laccolith itself is thought to be around 500 m (cf. Hawkes and Hawkes, 1933).

(Fig. 7). Perhaps the most common type of magma chamber, however, is sill-like (Figs. 7d, 8). This is the shape that is often imaged in seismic studies of volcanoes and rift zones, such as at mid-ocean ridges (Macdonald, 1982; Sinton and Detrick, 1992; Mutter et al., 1995; MacLeod and Yaouancq, 2000; Singh et al., 2006; Canales et al., 2009). This magma-chamber shape that is supported by the common occurrence of sills in volcanic areas and the formation of collapse calderas. Generally, a sill-like magma chamber is the geometry most favourable for the generation of the ring-faults along which piston-like subsidence takes place (Geyer et al., 2006; Acocella, 2007; Geyer and Marti, 2008, 2009; Gudmundsson, 2011a).

When certain mechanical conditions are satisfied, a sill may develop into a laccolith (Pollard and Johnson, 1973; Pasquare and Tibaldi, 2007; Bungler and Cruden, 2011). Some magma chambers are clearly laccoliths (Fig. 6). However, in general, laccoliths are much less

common than sills or larger plutons, so that we may assume that, even if magma chambers of such a geometry exist, they are not very common. Much more common are general oblate-ellipsoidal chambers (Fig. 7d). These are similar to sill-like chambers but, partly because of the size and density of the magma, the magma pressure may bend the layers above and below and forms a comparatively thick, oblate-shaped chamber. Many large chambers worldwide are apparently of this shape (Petraske et al., 1978; Sibbett, 1988; Marsh, 1989, 2000; Menand et al., 2011).

Bell-jar magma chambers have often been proposed for plutons and magma chambers (Anderson, 1936). A bell-jar intrusion is essentially a ring fault that fails to reach the surface and whose vertical parts connect through a subhorizontal fracture (for example, along an existing contact between lava flows). The idea is that magma is injected under the contact/roof and the host-rock below subsides

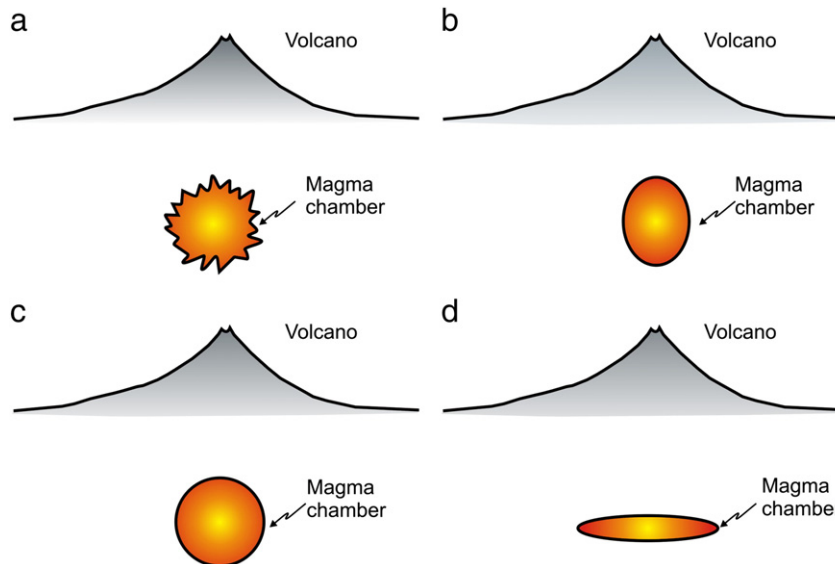


**Fig. 7.** Schematic illustration of the various possible shapes of magma chambers. (a) Chambers with very irregular boundaries (surfaces) are thermally and mechanically unstable and tend to smooth out the irregularities (cf. Fig. 9). (b) Roughly prolate ellipsoidal chambers may exist beneath some volcanic edifices, particularly comparatively narrow cones with steep slopes. This follows because the magma-chamber rupture, and associated feeder dykes, would mostly be injected from the top of the chamber, indicating a narrow surface area for the eruptions. (c) Roughly spherical magma chambers may be common, particularly at the later stages of the chamber evolution. Many such chambers generate swarms of inclined sheets. (d) Roughly oblate ellipsoidal or sill-like chambers are presumably the most common chamber geometry. They are particularly common at mid-ocean ridges, but have been detected seismically beneath many volcanoes.

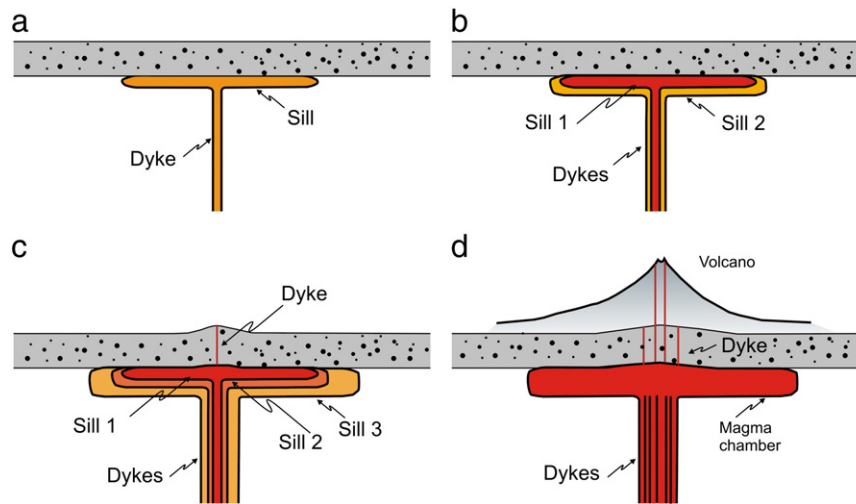


**Fig. 8.** Schematic illustration of a magma-chamber formation through the injection of sills. (a) A sill forms at the contact between mechanically dissimilar rock layers (cf. Menand, 2008, 2011; Gudmundsson, 2011b). (b) Subsequent dyke injections become arrested and their magmas partly absorbed by the original sill. (c) The sill cluster expands and (d) forms a sill-like magma chamber that supplies magma to a volcano. In this schematic illustration, the earlier sills are shown as cooling somewhat before a new sill emplacement occurs (sills number 1–3 in (c)). However, if the rate of injection is so low that the earlier sills solidify before the new injections occur, the cluster is unlikely to develop into a magma chamber and more likely to be recognisable as individual sills or a single sill with many columnar rows (Fig. 4). Here it is assumed that all the sills stay liquid during the formation of the chamber, even if they are shown as having cooled somewhat (the change in colour) between successive injections (c). This scenario is generally appropriate for both mafic and felsic sills, but in the latter case the sill contacts may still be seen even if the body acted as a single magma chamber (Fig. 5).

into an existing magma chamber below, in a similar manner as piston-like subsidence occurs along ring faults. A classic example of a bell-jar intrusion is the Great Eucrite Intrusion, of gabbro, forming a part of the intrusive complex of Ardnamurchan in West Scotland (O'Driscoll et al., 2006).

Bell-jar geometry has also been suggested for the Slaufudalur Pluton (Cargill et al., 1928). There is no doubt that the walls of Slaufudalur are faults (Fig. 5a), but there is no evidence that they acted as ring dykes (Gudmundsson, 2011b). Furthermore, as indicated above, there is clear evidence of forceful emplacement of the intrusion. The trend of the Slaufudalur Pluton is parallel with the palaeorift zone, so that the faults are likely to be steeply dipping normal faults. Slip on graben faults is known to change the stress field so as to encourage dyke deflection into sills (Gudmundsson, 2011a).

The evolution of the sills into a larger magma chamber is thus likely to be as follows (Fig. 8). A dyke becomes deflected into a sill at a contact where the mechanical properties and changes in local stresses favour sill formation (Gudmundsson, 1990, 2011b; Menand, 2008; Menand et al., 2011). If the dyke-injection frequency is so high that the earlier sills do not have a chance of solidifying before new dykes meet the sills, the dykes tend to be deflected again and again on meeting the earlier sills (Fig. 8b–c; Gudmundsson, 2011b). Subsequent sills are then emplaced (normally below) the earlier sills, thereby building up the magma chamber (Fig. 8d).

In case the dyke was injected into a graben, a recent slip on the graben faults would increase the horizontal compressive stress within the graben and thereby help trigger the dyke deflection into the sill. If the supply of magma is high enough, the sill propagates laterally until it meets with one or both the normal fault (Fig. 3e). Many sills in rift zones, such as in sedimentary basins, are known to terminate at normal faults (Fjeldskaar et al., 2008). Thus, it may be that many of the intrusions classified as bell-jar are simply piling up of sills within an active graben, as is likely to have been the case for formation of the Slaufudalur magma chamber (Fig. 5). Depending on the stress situation, some sills are able to propagate upwards (or downwards) along the fault for a while and then propagate laterally again (Fig. 3f). Most, however, terminate at the faults (Fig. 3e).

Some magma chambers eventually become spherical (Fig. 7c) or even prolate-ellipsoidal (Fig. 7b; Gudmundsson, 1988, 1990). A prolate-ellipsoidal chamber is most easily developed from cylindrical

conduits at shallow depths, perhaps at the intersections between major tectonic fractures. Fossil chambers of this shape are represented by plugs and necks, as are commonly seen at shallow depths in eroded stratovolcanoes.

Spherical magma chambers are favoured in volcanoes subject to an isotropic or close-to isotropic state of stress (Fig. 7c). But this geometry may also result directly from the cooling of a chamber that originally had a different shape. When the rate of receiving new magma does not keep up with the rate of cooling and solidification, the size of the fluid part of the magma chamber reduces. To minimise the rate of flow of heat out of the chamber, it may gradually evolve into a spherical chamber (Fig. 7c). An original sill-like, oblate spheroidal or prolate spheroidal magma chamber may (Fig. 7), when the heat supply decreases, may change into a comparatively small, spherical magma chamber. Thus, many spherical chambers may be remnants of earlier and larger chambers of different shapes. It is, however, also possible that some very long-lived large magma chambers become close to spherical in shape, particularly if the time-average regional state of stress is close to isotropic. This would be partly achieved through forceful up-bending and down-bending of the host-rock layers above and below the chamber, and partly through anatexis (melting) and perhaps some ductile deformation, of the host rock.

A long-lived magma chamber cannot be very irregular in shape; it tends to smooth out the initial surface irregularities during its lifetime (Fig. 9). Thus, fossil magma chambers, plutons, tend to have comparatively smooth large-scale contacts with the surrounding rocks (Figs. 5, 10a), even if some show evidence of complex interaction between different magmas (Fig. 10b). That large-scale irregularities in contacts tend to smooth out follows from simple thermal considerations (Jaeger, 1961, 1964; Gudmundsson, 1990). For example, if an irregular part of the chamber projects into the host rock, that part has a comparatively large area of contact with the host rock, so that, assuming that the host rock is cooler than the magma (as is normally the case), heat is transferred rapidly from the magma to the host rock. This part of the chamber tends to cool down rapidly, become solidified, and thus no longer a part of the active chamber. Conversely, if an irregular part of the host rock projects into the magma chamber, heat is transferred rapidly from the magma into that part of the host rock which, thereby, tends to melt partially. Eventually, the

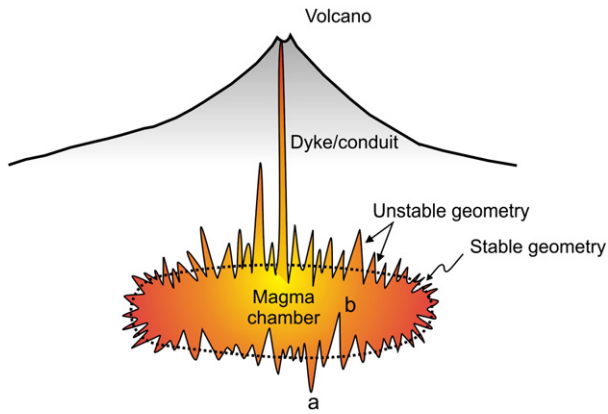


**Fig. 9.** Magma chamber with a very irregular boundary (surface) is mechanically and thermally unstable. It is mechanically unstable because the notches that project into the host rock are stress raisers and would inject dykes if there was any non-zero excess pressure in the chamber. It is thermally unstable because the jogs that project into the chamber would tend to melt, and the notches that project into the host rock would tend to solidify. Gradually, the chamber would assume a more stable, smoother geometry, as indicated; commonly, similar to that in Fig. (18).

whole part of the host rock may melt when it breaks off from the main part of the roof or the walls, and subsides into the chamber (a process referred to as stoping).

Many hydrocarbon reservoirs are compartmentalised, that is, are composed of domains or parts (compartments) that are mechanically different from the adjacent parts or domains (Economides and Nolte, 2000; Satter et al., 2008). For hydrocarbon reservoirs, compartments are commonly domains with different pore-fluid pressures, so that the pressures in adjacent parts of the reservoir may be quite different. The compartmentalisation is often related to tight faults, that is, faults with very low permeability that separate different parts of the reservoir so that there is no fluid flow between the adjacent parts.

Totally fluid magma chambers composed of a single magma type cannot normally be compartmentalised. This follows because compartments in the present sense can only arise if there are some physical boundaries, such as contacts or faults, that hinder the free flow of material (here fluids) in response to pressure/hydraulic gradients between different parts of the chamber. However, many magma chambers contain magmas of very different compositions with widely different thermal and mechanical properties. Furthermore, the magmas in a chamber are generally at various stages of solidification and thus at a different temperature and viscosity. For example, on the top of a totally molten basaltic magma chamber there may be partially molten, or solidified, acid magma that may be injected by basaltic dykes and inclined sheets. Basaltic sheets, for example, dissect some of the granophyre layers in the fossil chamber of Slaufudalur (Fig. 5). It is not known exactly at what time these injections took place, but some of them may have been intruded while the granophyres magma was still partially molten and behaving as poroelastic. In the latter case, the basaltic sheets could have formed barriers for lateral fluid transport between nearby granophyric parts, thereby forming compartments.

Similar compartments, but on a much smaller scale, are common in magma chambers and exemplified by net-veined complexes (Fig. 10). Any rock bodies with a low permeability and different mechanical properties from the adjacent parts of the magma chamber may function as a temporary or permanent barriers to fluid transport and mixture, and thus contribute to the generation of compartments (a detailed discussion of magma-chamber compartments is in Section 7).

#### 4. Crustal stresses

Stress is a measure of the intensity of force per unit area. That is, the greater the intensity of the force for a given area on which the

force acts, the greater is the stress. In the simplest way, stress may be defined as:

$$\sigma = \frac{F}{A}. \quad (1)$$

Here  $F$  is the force in newtons (N) and  $A$  is the area in square metres ( $\text{m}^2$ ) upon which the force acts. The symbol  $\sigma$  is used, as I do here, when the force that generates the stress is normal to the area  $A$  upon which it acts and is referred to as normal stress. By contrast, a shear force operates parallel to the plane of interest, such as a fault plane, and generates shear stress. Shear stress is here denoted by the symbol  $\tau$ .

The units of stress are  $\text{Nm}^{-2}$ , that is, newtons per square metre, referred to as pascals. A pascal, however, is a very small unit, roughly equal to the pressure given by water lens of thickness  $1 \times 10^{-4}$  m or 0.1 mm. Thus, in geology and many other sciences megapascals (million pascals) are used for stress and pressure and strength, and gigapascals (thousand million pascals) for elastic moduli (such as Young's modulus and shear modulus) of the rock units and layers.

Stress as defined in Eq. (1) is a vector, sometimes referred to as the traction, the traction vector, or simply the stress vector. It is a vector because the product of a vector (here force) and a scalar (here the reciprocal of area) is a vector (and, also, because the orientation of the surface on which it acts is assigned a priori). At a point in the earth's crust, however, there act numerous stress vectors, and the three-dimensional collection of all these vectors, for the (fracture or contact or imaginary) planes of all possible attitudes at that point, define the stress tensor. Thus, the state of stress at a point in the earth's crust is a second-order tensor, or simply a tensor, the orientation of the surface on which it operates not being assigned a priori. The component of stress in any particular direction, however, is a vector. In physics, engineering, and particularly in geosciences it is common to refer to the stress in a given direction, such as the stress on a fault plane or stress on a crystal slip plane. In this paper, the term traction is not used. Instead, the word stress is used both for the stress vector and the stress tensor. Also, compressive stress is regarded as positive and tensile stress as negative, as is common in geosciences.

The geostatic stress, or vertical stress, is given by:

$$\sigma_v = \int_0^z \rho_r(z)g dz \quad (2)$$

for the case of crustal layers with different densities, that is,  $\rho(z)$ , or as:

$$\sigma_v = \rho_r g z \quad (3)$$

for the case where all the crustal layers have the same density, namely  $\rho_r$ . Here, the vertical coordinate  $z$  is positive downwards, that is, towards increasing crustal depth, and  $g$  is the acceleration due to gravity. Geostatic stress is also referred to as overburden pressure which, however, is more appropriately identified with lithostatic stress (or pressure). The three concepts, geostatic stress, overburden pressure, and lithostatic stress/pressure, are used interchangeably in the geoscience literature. Here I shall mainly use lithostatic stress with the following definition.

For any stress state at a point in the crust, there are three mutually orthogonal planes that are free of shear stress. These are named the principal stress planes and the normal stresses that act upon these planes are known as the principal stresses. The three principal stresses are denoted by  $\sigma_1$ ,  $\sigma_2$ , and  $\sigma_3$ , with the maximum compressive principal stress being  $\sigma_1$ , the intermediate principal stress being  $\sigma_2$ , and the minimum principal compressive (maximum tensile) principal stress being  $\sigma_3$  (e.g., Jaeger et al., 2007; Gudmundsson, 2011a).

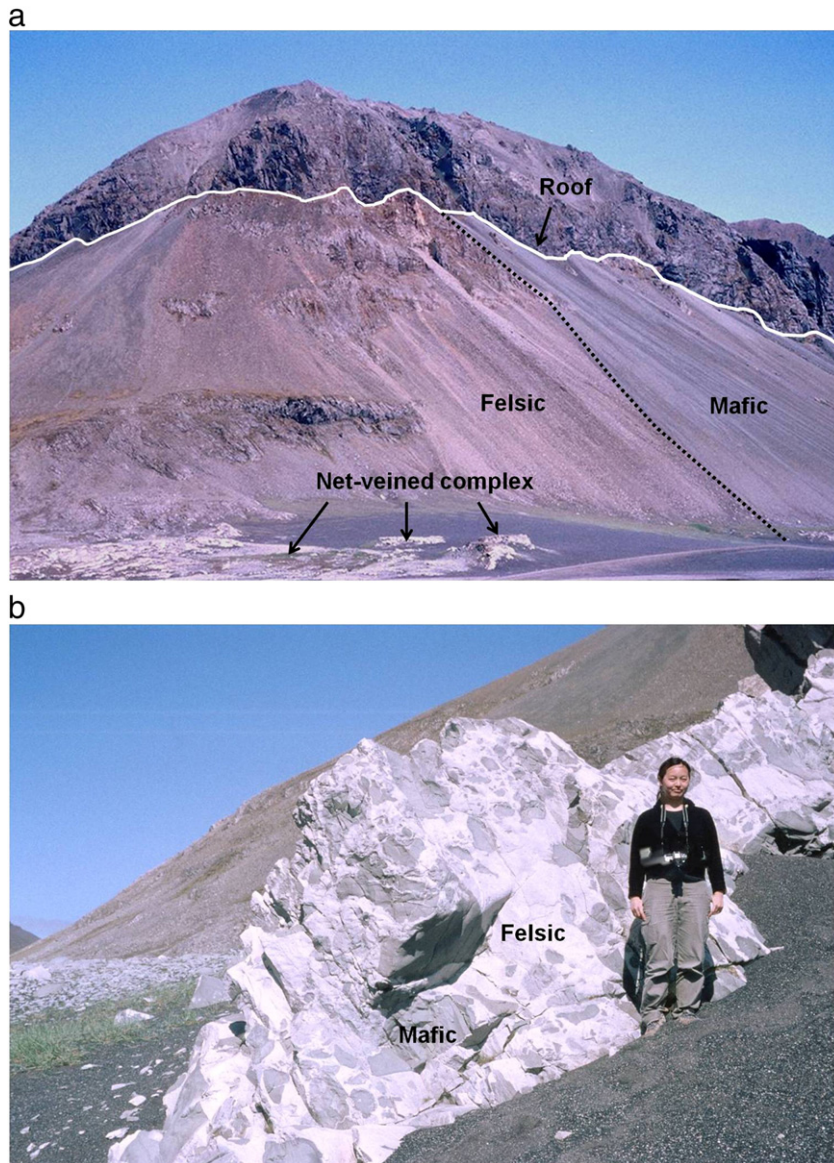


**Fig. 10.** Large-scale contacts between plutons and their host rocks tend to be smooth, as indicated by the roof of a part of the Austurhorn Pluton, a fossil magma chamber in South-east Iceland (Blake, 1966; Furman et al., 1992). The same plutons may show evidence of very complex small-scale interaction between widely different magmas, forming small-scale 'compartments' of so-called net-veined complexes. (a) Part of the roof of the Austurhorn Pluton, here exposed in the mountain Krossanesfjall (its height is 716 m). Also indicated are the comparatively smooth contact between the pluton and its roof and the contact between the primarily felsic and primarily mafic intrusions in part of the mountain. On the sandy coast, a part of the net-veined complex in Krossanesfjall is seen. (b) Close-up of the part of the complex seen on the flat ground close to the road in the photograph in (a). The very light-coloured rocks are felsic, the grey to dark rocks being mafic.

If all the principal stresses are equal (isotropic or hydrostatic or spherical state of stress) and the stress magnitude increases with depth as in Eq. (3), then the state of stress is referred to as lithostatic. While deviation from lithostatic stress is associated with unrest periods, lithostatic stress is usually used as a reference state of stress for magma chambers. This follows because, except during unrest periods, the magma-pressure is likely to be close to the pressure or stress in the host rock, that is, to be in a lithostatic equilibrium. For a host rock that behaves as elastic, as the earth's upper crust generally does during unrest periods (e.g., Mogi, 1958; McTigue, 1987; Dzurisin, 2006; Segall, 2010), the host rock responds immediately to pressure changes in the chamber. If the pressure increases, that is, if there is an excess pressure (pressure above lithostatic—see a more detailed definition in Section 5) in the chamber, the chamber expands (resulting in an inflation). If, eventually, the excess pressure reaches the tensile strength of the host rock the chamber ruptures and injects

dykes, inclined sheets, or sills. If the excess pressure decreases, that is, if the chamber volume decreases, the chamber shrinks (resulting in a deflation), so as to establish close-to-lithostatic pressure again. Thus, unless some considerable inflow (replenishment) or outflow of magma or other pressured fluids is taking place, the long-term mechanical condition of a magma chamber is that of lithostatic equilibrium with the host rock.

##### 5. Stresses and pressures associated with dykes and sills

The lithostatic equilibrium of a magma chamber may become disturbed during external and/or internal loading, as normally happens during unrest periods. Loading here means forces, stresses, pressures, or displacements acting applied to a body such as a magma chamber. As mentioned, most magma chambers originate from sills and many remain sill-like throughout much of their life-times (Figs. 7d, 8, 9).

Also, sills are normally fed by dykes. It is therefore appropriate to start our analysis of stress around magma chambers by considering stress-ess around sills and dykes.

Consider first the emplacement of a sill, that is, the deflection of a dyke into a sill (Figs. 3, 8; cf. Gudmundsson, 2011b). For a pure hydrofracture such as a dyke, the fracture path is opened by overpressure (driving pressure, net pressure) of the magma. It is this overpressure that drives all hydrofractures open, including man-made hydraulic fractures used for crustal stress measurements and in the geothermal and petroleum industries to increase the permeability of reservoirs (e.g., Hubbert and Willis, 1957; Sneddon and Lowengrub, 1969; Sun, 1969; Daneshy, 1978; Warpinski, 1985; Spence et al., 1987; Lister and Kerr, 1991; Rubin, 1995; Valko and Economides, 1995; Amadei and Stephansson, 1997; Yew, 1997; Economides and Nolte, 2000; Zoback, 2007; Zang and Stephansson, 2010).

For the dyke to form and propagate, the magmatic overpressure must be sufficiently high to overcome the tensile strength of the host rock  $T_0$  and the normal stress on the magma-filled fracture, that is, the dyke fracture. Field observations, primarily cross-cutting relations, show that most dykes and sills (and inclined sheets) are extension fractures. This means that the fracture forms in a plane that contains two of the principal stresses, namely the maximum and the intermediate stresses  $\sigma_1$  and  $\sigma_2$ . That plane, by definition, is perpendicular to the minimum principal stress  $\sigma_3$  (Fig. 11). When a dyke forms, the state of stress is normally anisotropic, that is, non-lithostatic, so that the principal stresses are unequal. Because most dykes are emplaced in rift zones, the normal state of stress is such that  $\sigma_3$  is sub-horizontal and perpendicular to the strike dimension of the forming dyke,  $\sigma_2$  is also sub-horizontal and parallel with the strike of the dyke, and  $\sigma_1$  is sub-vertical and parallel with the dip dimension of the dyke (Fig. 11). This state of stress is the normal one during rifting events at divergent plate boundaries.

The vertical stress  $\sigma_1$  is given by Eqs. (2), (3) and clearly includes the effects of the acceleration due to gravity  $g$ . In fact, the vertical stress given by Eq. (3) follows directly from the acceleration due to gravity,  $g$ , and the definition of stress as given in Eq. (1). In Newton's second law of motion, force is defined as mass times acceleration ( $F = m \times a$ ). Close to the Earth's surface, the acceleration  $a$  in the Earth's gravity field is  $g$  (on average,  $9.81 \text{ m s}^{-2}$ ), in which case the second law may be written as:

$$F = m \times g. \quad (4)$$

The mass  $m$  of a rock particle or body is equal to the body's volume times its density. For a rock column of unit cross-sectional area, say close to a dyke (Fig. 12), the volume must be the unit area  $A$  times the crustal depth  $z$ . With  $A = 1$ , the volume is  $z$  (in units of  $\text{m}^3$ ), and we have:

$$\sigma_1 = \frac{F}{A} = \frac{mg}{A} = \frac{\rho_r z g}{1} = \rho_r g z. \quad (5)$$

Here the vertical stress (for a rift zone) is assumed to be the maximum principal stress  $\sigma_1$ . In an extensional regime, such as at a divergent plate boundary or a rift zone, the horizontal stress (here  $\sigma_3$ ) is related, theoretically, to the vertical stress (here  $\sigma_1$ ) through the following equation (Fyfe et al., 1978):

$$\sigma_3 = \frac{\nu \sigma_1}{1 - \nu} = \frac{\sigma_1}{m - 1} \quad (6)$$

where  $\nu$  is Poisson's ratio,  $m = 1/\nu$  is Poisson's number (the reciprocal of Poisson's ratio), and the other symbols are as defined above. Eq. (6)

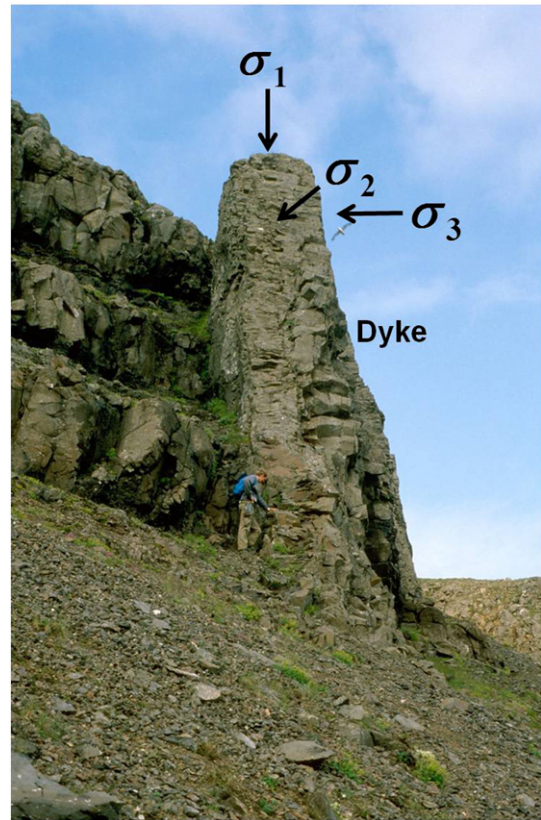


**Fig. 11.** State of stress encouraging the emplacement of a dyke. The vertical stress is the maximum principal compressive stress,  $\sigma_1$ , the horizontal stress parallel with the trend/strike of the dyke is the intermediate principal compressive stress,  $\sigma_2$ , and the horizontal stress perpendicular to the dyke is minimum principal compressive (maximum tensile) stress,  $\sigma_3$ . Here, a 2.5-m thick basaltic dyke from the Quaternary lava pile (a palaeorift zone) in Southwest Iceland. When the dyke becomes emplaced, it may, temporarily, change the normal stress field so as to encourage the subsequently emplaced dyke to become deflected into a sill (Figs. 1, 3, 8).

assumes that the horizontal strains (here  $\epsilon_3 = \epsilon_2$ ) in the host rock are zero. When that is not the case, Eq. (6) is commonly rewritten as (Fyfe et al., 1978):

$$\sigma_3 = \frac{\sigma_1}{m - 1} \pm \epsilon_3 E \quad (7)$$

where  $E$  is Young's modulus.

Eqs. (6) and (7) make many assumptions, most of which are listed by Gudmundsson (2011a, p. 112). The equations be applied to estimate the tensile stress close to a totally molten magma chamber, or other fluid-filled reservoirs, because, using a common value of Poisson's ratio of 0.25 (Carmichael, 1989; Hansen, 1998; Bell, 2000; Myrvang, 2001), the minimum theoretical principal stress would be about one-third of the maximum principal stress, or:

$$\sigma_3 = \frac{1}{3} \sigma_1 \quad (8)$$

and such a stress difference is normally not possible to reach in the vicinity of a rock-magma (or other fluid) contact. For a magma chamber initially in a lithostatic equilibrium, long before  $\sigma_3$  could be reduced to  $1/3\sigma_1$ , a hydrofracture (a dyke, an inclined sheet, or a sill) would be injected and the stress difference reduced (Gudmundsson, 2006).

Eqs. (6)–(8) together with Eqs. (2)–(5) show that the effect of gravity, through the acceleration  $g$ , is always included in the calculations. As a consequence, most authors do not consider the total pressure in a magmatic intrusions or a magma chamber when analysing the stresses around these structures but rather the excess pressure

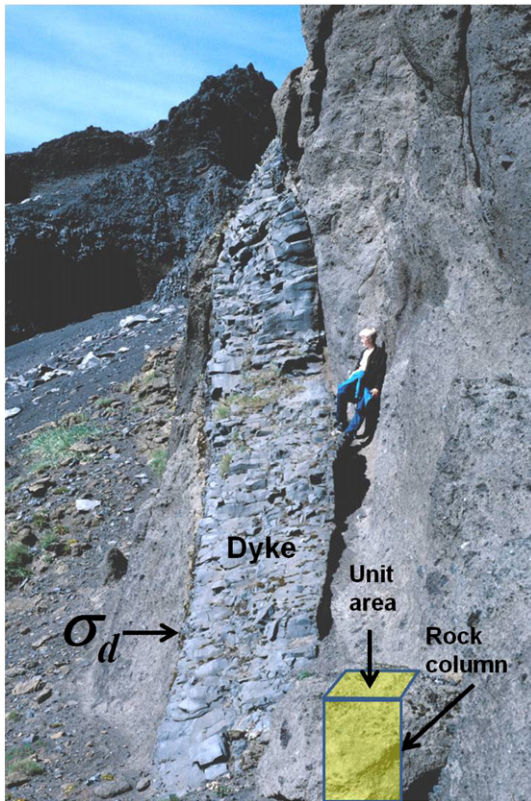


**Fig. 12.** State of stress in the crust close to a dyke, with reference to Eqs. (2), (3), (5), and (12). The unit cross-sectional area of a rock column used is indicated, as well as the differential stress  $\sigma_d$  at the crustal level where the dyke is measured, and used in Eq. (12). The depth of the unit area below the earth's surface at the time of dyke emplacement is  $z$  in Eqs. (2), (3), and (5), whereas the height of the dyke exposure above the magma source (the dyke dip dimension) is  $h$  in Eq. (12).

or the overpressure. The main pressure concepts may be defined as follows (Gudmundsson, 2011a):

- (1) Excess pressure ( $p_e$ ) in a magma chamber (or other hydrofracture sources) is the magma pressure in excess of the lithostatic pressure (or overburden pressure), that is, the total pressure (defined below) minus the lithostatic pressure. Excess pressure at the time of rupture and hydrofracture formation is normally equal to the tensile strength of the host rock of the reservoir and thus generally in the range of 0.5–6 MPa, with a maximum of about 9 MPa, and most commonly about 3 MPa.
- (2) Overpressure ( $p_o$ ) – also named driving pressure and net pressure – is the pressure that drives the propagation of a hydrofracture (a fluid-driven extension fracture), such as a dyke, a sill, or an inclined sheet. Overpressure is the result of the combined effects of the initial excess pressure in the magma chamber and the magma buoyancy, the latter being due to the difference between the density of the fluid in the fracture and the density of the rock through which the fracture propagates. It is the total pressure minus the normal stress which acted on the potential sheet (dyke or sill) fracture before magma emplacement; for a hydrofracture the normal stress is the minimum principal compressive stress  $\sigma_3$ . The excess pressure decreases along the flow direction in the fracture: for example, up the dip-dimension of a sub-vertical dyke. By contrast, the buoyancy term increases so long as the average density of the host-rock through which the fracture propagates is greater than the density of the fluid (here magma). The overpressure may reach several tens of megapascals at some point

along the dyke path even though the excess pressure at the fluid source is normally equal to the rock tensile strength and thus only several megapascals.

- (3) Total pressure ( $p_t$ ) in a magma chamber is its excess pressure plus the lithostatic stress (or overburden pressure). When a magma chamber is in a lithostatic equilibrium with its host rock, that is, in the absence of unrest, there is normally no tectonic activity associated with the chamber, such as hydrofracture initiation or faulting. It is only when there is some (usually positive, but occasionally negative) excess pressure in the reservoir that stresses build up in the surrounding rocks which, eventually, may result in faulting or hydrofracture initiation.

The conditions for hydrofracture initiation from a fluid source are sometimes given using the total pressure, namely as (Jaeger et al., 2007):

$$p_t = \sigma_3 + T_0 \quad (9)$$

where  $T_0$  is the in situ tensile strength of the host rock, and the other symbols are as defined above. Eq. (9) may be used for dykes (and sills and inclined sheets), but is most useful for the initiation of hydraulic fractures injected from drill holes (Valko and Economides, 1995; Amadei and Stephansson, 1997; Yew, 1997; Economides and Nolte, 2000; Zoback, 2007; Zang and Stephansson, 2010). Because the total pressure is equal to the excess pressure plus the lithostatic pressure, we have:

$$p_t = p_l + p_e \quad (10)$$

so that, using Eq. (9), we can write Eq. (10) in the form:

$$p_l + p_e = \sigma_3 + T_0 \quad (11)$$

where  $p_l$  is the lithostatic stress at the rupture site in the walls of the magma chamber,  $p_t$  is the total magmatic pressure in the chamber,  $\sigma_3$  is the minimum principal stress, and  $T_0$  the local in situ tensile strength at the rupture site. If a dyke (or an inclined sheet) becomes injected into the roof of the chamber and starts to propagate up into the crustal layers above the chamber, the magmatic overpressure  $p_o$  in the dyke is given by:

$$p_o = p_e + (\rho_r - \rho_m)gh + \sigma_d \quad (12)$$

where  $\rho_r$  is the average host-rock density,  $\rho_m$  is the average magma density,  $g$  is acceleration due to gravity,  $h$  is the dip dimension or height of that part of the dyke above the point of rupture and dyke initiation, and  $\sigma_d$  is the differential stress ( $\sigma_d = \sigma_1 - \sigma_3$ ) at the level where the dyke is examined (Fig. 12).

Eq. (12) can be used to estimate the likely overpressure of a dyke that has reached a certain elevation (height or dip dimension) in the crustal layers above its magma chamber (Figs. 1, 3, 11–14). When using Eq. (12), however, the following should be considered:

- (1) At the time of dyke initiation from a reasonably large magma chamber, the excess pressure  $p_e = p_m - p_l$  is, as a rule, positive, as is needed to rupture the chamber walls. Normally, when the excess pressure reaches roughly the tensile strength, in which case  $p_e = T_0$ , the reservoir ruptures in tension and a dyke (or an inclined sheet or a sill) initiates.
- (2) The differential stress, defined as  $\sigma_d = \sigma_1 - \sigma_3$ , is either zero or positive (Fig. 12); it cannot be negative because  $\sigma_1 \geq \sigma_2 \geq \sigma_3$  so that  $\sigma_1$  cannot be less than  $\sigma_3$ . When  $\sigma_d = 0$ , then  $\sigma_1 = \sigma_3$  so that the state of stress is isotropic (here in two dimensions) and when applied to three dimensions (so that we also have  $\sigma_1 = \sigma_2$ ), then the state of stress is lithostatic.

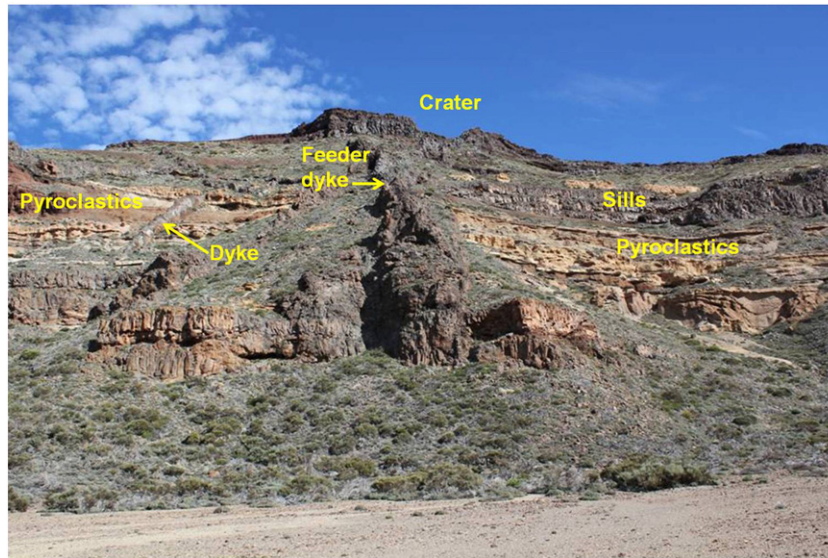


**Fig. 13.** High-density basaltic feeder-dyke passing through many low-density pyroclastic rocks (some layers are indicated) in the caldera wall of Las Canadas in Tenerife (Canary Islands). View east, the caldera wall is close to 300 m high. Part of the same feeder dyke is seen in Fig. 4b. Several other basaltic dykes and sills are seen in the section.

- (3) The density difference  $\rho_r - \rho_m$  can be (1) negative, when the magma is denser than rock; (2) zero, when the density of the magma is equal to that of the rock; or (3) positive, when the rock is denser than the magma. The density of most crustal rocks is in the range of  $2000 \leq \rho_r \leq 3000 \text{ kg m}^{-3}$  (Carmichael, 1989; Hansen, 1998; Bell, 2000; Schon, 2004) whereas that of typical magmas is mostly in the range  $2250 \leq \rho_r \leq 2750 \text{ kg m}^{-3}$  (Murase and McBirney, 1973; Kilburn, 2000; Spera, 2000).

When dealing with stresses around magma chambers and dykes and other sheet intrusions, it is the excess pressure (for the chamber) and the overpressure (for the dyke) that is important for brittle deformation. The total pressure is rarely used. It follows from the analysis and equations above that the effects of gravity are automatically taken into account in such an analysis.

Since dykes injected from magma chambers feed most eruptions, let us briefly consider the conditions for feeder-dyke formation and, in particular, the effect of ‘neutral buoyancy’ on the chance of the dyke reaching the surface. For dyke initiation, Eqs. (9) or (11) must be satisfied. At its initiation, there is no buoyancy effect on the magma pressure because  $h$ , the height or the dip dimension of the dyke as given in Eq. (12), is zero. However, as the dyke propagates upwards into the crustal layers above the roof of the chamber, its dip dimension  $h$  gradually increases, so that buoyancy, as presented by the second term on the right-hand side of Eq. (12), adds to its initial excess pressure  $p_e$  so as to generate the overpressure  $p_o$ . The buoyancy effect depends on the density difference between the magma and the host rock. If they are of equal density, on average, then the buoyancy effect remains zero. If the magma is denser than the average density of the crustal layers through which the dyke

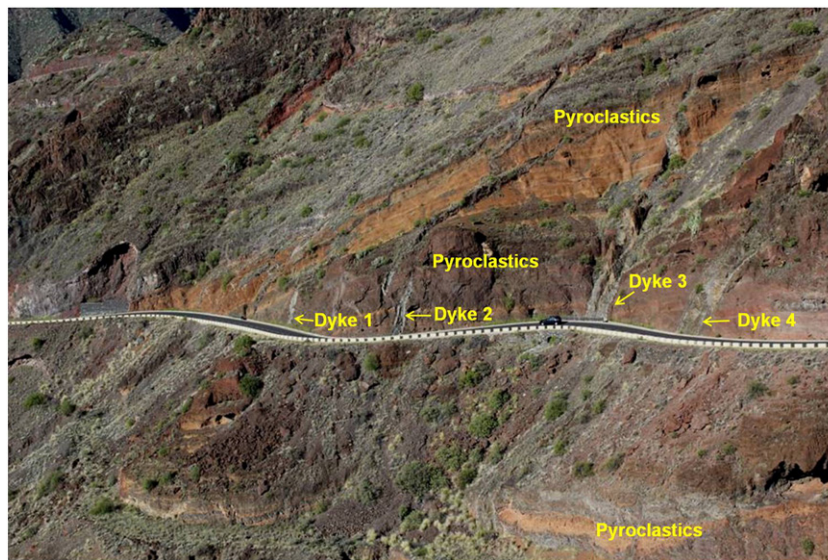


**Fig. 14.** Many basaltic dykes pass easily through low-density pyroclastic rocks (some layers are indicated) in the peninsula of Anaga, Tenerife (Canary Islands). Comparatively low density of layers, or a density similar to that of the magma (‘neutral buoyancy’), is normally not sufficient to arrest propagating basalt dykes. Dykes 1 and 2 are 1–2 m thick, and dykes 3 and 4 both around 5 m thick. A black car close to Dyke 3 also provides a scale.

propagates, then the buoyancy effect is negative, so that the excess pressure at the rupture gradually decreases with height above the chamber. If, however, the rock is denser than the magma, then buoyancy effect is positive and the magmatic overpressure increases with increasing dip dimension  $h$  as the dyke propagates towards the earth's surface.

The average density of the uppermost crustal layers through which a dyke (or an inclined sheet) propagates is commonly similar to or less than that of a basaltic magma (Figs. 13, 14). And, generally, the average density of the uppermost several hundred metres of the crust of a volcano-tectonically active rift zone is everywhere less than that of typical basaltic magma. The basaltic magma may have densities between  $2600 \text{ kg m}^{-3}$  and  $2750 \text{ kg m}^{-3}$ , whereas the uppermost crustal layers may have densities as low as  $2500 \text{ kg m}^{-3}$ , even in a predominately basaltic crust (e.g., Gudmundsson, 1988, 2011a). Thus, to reach the surface, basaltic magma almost always has to propagate through crustal layers of densities that are less than that of the magma. The basaltic magma has normally to propagate through many layers where the buoyancy is zero, so-called 'levels of neutral buoyancy', or even negative (Figs. 13, 14). This follows because typical rift zones are composed of a variety of rocks. Even a predominantly basaltic crust usually contains numerous layers of breccias, pyroclastics (hyaloclastites), sediments, intrusions and other rocks with different densities (Figs. 13, 14). Thus, for a basaltic dyke propagating through such a pile, there are normally many layers of densities equal to that of the magma at a particular location (the magma density also changes with elevation in the dyke/conduit because of degassing and other processes). Generally, therefore, there are many 'levels of neutral buoyancy' for a basaltic magma on its way to the surface (Fig. 13).

A 'level of neutral buoyancy' has often been suggested as a trap for basaltic magma, so as to either arrest dykes or deflect them into sills—and thereby generate potential magma chambers (Bradley, 1965; Holmes, 1965; Gretener, 1969; Francis, 1982; Ryan, 1993; Chevallier and Woodford, 1999). As we have seen, however, basaltic dykes pass easily through layers of densities less than those of typical basaltic magmas (Figs. 4, 13, 14). This is seen everywhere in the world where basaltic volcanism takes place. Most of this volcanism is supplied with magma through dykes, and all these dykes must pass through (usually many) 'neutral buoyancy' layers on their paths to

the surface. In fact, as indicated above, the top crustal layers at all divergent plate boundaries worldwide have densities less than those of typical basaltic magmas. Nevertheless, basaltic dykes or sheets pass through these layers to reach the surface in every single basaltic eruption. Thus, clearly, dykes do not as a rule change into sills at levels of neutral buoyancy; and neutral buoyancy layers/units do not stop the vertical propagation of the dykes.

Mechanically, there are no particular reasons why dykes should stop, change into sills, or propagate laterally at levels of neutral buoyancy. From Eq. (12) it follows that, for a gradually increasing average host-rock density with increasing crustal depth (as is commonly crudely the case), the highest magmatic overpressure occurs at the 'regional' level of neutral buoyancy. So, unless the local stress field, the tensile strength, or toughness of the rock change abruptly at the contact with the level of neutral buoyancy, there is all the reason for the dyke to continue its subvertical propagation path—that is, to propagate though the level of neutral buoyancy. And this is, indeed, what is observed in the thousands of basaltic dykes that propagate through layers of much lower densities, such as layers of basaltic breccias (hyaloclastites), ignimbrites, and rhyolites (Figs. 4, 13, 14).

## 6. Stresses around magma chambers

### 6.1. Stresses at magma-chamber initiation

We have considered the deflection of a dyke into a sill and seen that when we work with overpressure (net pressure, driving pressure) the analysis automatically considers the effects of gravity, as indicated in Eqs. (2)–(7). For a sill (or a dyke) to form, the conditions of Eqs. (9) or (11) must be satisfied. For a sill, the minimum principal compressive stress,  $\sigma_3$ , is vertical and given by Eqs. (2) or (3). The stress is the same on the roof of the sill as on the rocks just ahead of its tips. Similarly, for a magma chamber in lithostatic equilibrium, the vertical stress on the roof of the chamber is the same as that, at the same crustal level and for the same rock density, just outside the roof.

Consider the fossil magma chamber in Fig. (5a). If the vertical stress on the roof of the chamber at, say, point A is given by Eqs. (2) and (3), then, if point B is at the same crustal depth as point A and the rock density in the columns above these points is the same (and the chamber is in lithostatic equilibrium), the vertical stress at point B must be the same as at point A. If the magma density equals the rock density (which may or may not have been the case in Fig. 5), then it follows that the increase in vertical stress with depth from point A is also given by Eq. (3) and the same applies to the vertical stress along the chamber wall below point B.

Lets for a moment see what the consequences would be for a sill formation or magma-chamber development if the vertical wall-parallel stress at B and parallel with the wall of the fossil chamber was much higher, say double, the vertical stress on the top of the magma chamber. Now the exposed fossil chamber is composed of sills (Fig. 5b), so that the top part in Fig. (5a) is a sill. In this scenario, we have  $2\sigma_v$ , that is, for the sill,  $2\sigma_3$ , acting on the rock at point B but  $\sigma_3$  at point A (Fig. 5b). The sill had to propagate from its feeder dyke (Figs. 3, 8), so that point B is always in the rock-wall just ahead of the propagating sill tip. This means that the vertical stress  $\sigma_v$  must suddenly change from  $\sigma_3$  on the top (the roof) of the sill to  $2\sigma_3$  just ahead of the tip of the sill.

But this would mean that the sill could not propagate at all. On the top of the sill the vertical stress, given by Eq. (3), is in balance with the magmatic pressure in the sill and the opening or aperture of the sill is entirely due to its overpressure as given, for example, by Eq. (12). These results are well known elastic crack theory (Sneddon and Lowengrub, 1969; Gray, 1992; Tada et al., 2000) and confirmed by numerous hydraulic fracture experiments worldwide (Valko and Economides, 1995; Amadei and Stephansson, 1997; Yew, 1997;

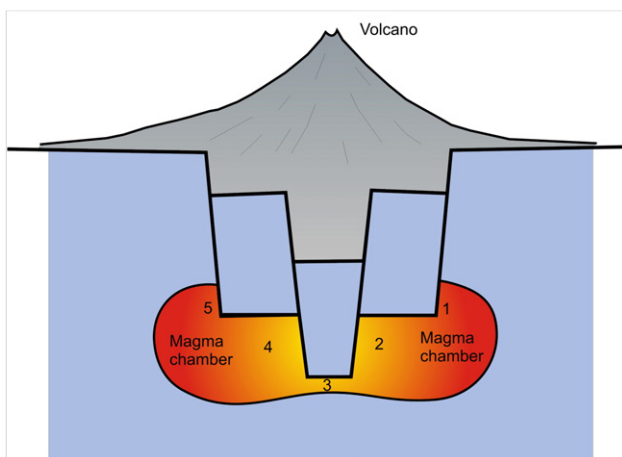


**Fig. 15.** Compartments in a magma chamber may be generated through faulting, for example the formation of (here nested) collapse calderas (for the formation of nested calderas see Geyer and Marti, 2009). Flow of magma between compartments 1 and 5, and 2 and 4 is unlikely since the magma would then first have to flow through compartment 3. Density differences between the magma in the upper part of the chamber and in its lower part make such a flow unlikely. For the same reason, flow between compartments 1 and 2, and 5 and 4 is likely to be minimal if any. The magma in each of the compartments may therefore, for a while at least, evolve largely independently of the magmas in the other compartments.

Economides and Nolte, 2000; Zoback, 2007; Zang and Stephansson, 2010). So it is only the overpressure that drives the sill. This overpressure has only to overcome the tensile strength of the rock, according to Eqs. (9)–(11).

For a typical basaltic sill, the overpressure at a few kilometre depth might be 10–20 MPa. Take, as an example, a sill emplaced at the depth of 3 km in the crust, a depth where many shallow magma chambers form. For the upper part of a typical crust at a divergent plate-boundary, the rock density is, on average, about  $2600 \text{ kg m}^{-3}$  (Gudmundsson, 1988), in which case the vertical stress, from Eq. (3) is about 76 MPa. For a sill, the overpressure is the total pressure minus the minimum principal compressive stress  $\sigma_3$ , here the vertical stress  $\sigma_v$  according to Eq. (3), namely 76 MPa. If the overpressure is 20 MPa, then the total magmatic pressure in the sill is 96 MPa.

If total vertical stress at the lateral tip or edge of the sill suddenly changes to  $2\sigma_3$ , then, in this case, it becomes 152 MPa. Since  $96 - 152 = -56$  MPa, it follows that the potential overpressure is less than zero, that is, negative ( $-52$  MPa), so that there is absolutely no overpressure in the sill, which means that it could not form in the first place, let alone propagate to form a magma chamber. This brings us to a recent model on the stress field around magma chambers that includes extra wall-parallel stress.

## 6.2. Different approach to magma-chamber stress modelling

The authors of several recent papers (Grosfils, 2007; Hurwitz et al., 2009; Long and Grosfils, 2009) have suggested that standard analytical elastic solutions for stress fields around magma chambers, such as those by Davis (1986), McTigue (1987), Tait and Jaupart (1989), De Natale and Pingue (1993), Saunders (2001), Gudmundsson (2002, 2006), Pinel and Jaupart (2003), and Masterlark (2007) as well as similar viscoelastic solutions (Bonafede et al., 1986; Folch et al., 2000; Trasatti et al., 2005) are 'correct but incomplete'. The solutions proposed by the authors themselves differ from those of almost all previous solutions in three important respects, namely as regards the following points (e.g., Grosfils, 2007):

- (1) They add an extra 'wall-parallel component of the lithostatic stress' which is also supposed to 'resist rupture' of the magma chamber walls (and thus dyke, sheet, or sill injection from the chamber). It follows that there is 'an important depth-dependent factor which also resists the rupture process'.
- (2) In some of their models the tensile strength of the rock hosting the magma chamber is taken as zero at the point of failure. This implies that the magma excess pressure at that point must be zero.
- (3) They claim that 'a magma chamber can support a wide range of uniform pressures  $P$  prior to the initiation of tensile failure. This result is certainly at odds with studies that claim that failure will occur when  $P$  rises to at most only a few MPa above the lithostatic'. In Table 1 of Grosfils (2007) the  $P$ -values in magma chambers before failure [uniform pressures; here excess magmatic pressures before rupture] are predicted to range up to hundreds of megapascals.

Here we discuss these three main points and the associated model, referred to as the EWS (extra wall-stress) model. All the references are to the principal paper by Grosfils (2007) unless otherwise stated.

### 6.2.1. The first point

In the EWS model, the first reference state of stress is lithostatic, that is,  $\sigma_1 = \sigma_2 = \sigma_3$  or, in the EWS-model notation  $\sigma_r = \sigma_\theta = \sigma_z$ , and the stresses increase in magnitude according to Eqs. (2) and (3). For this reference state, it is assumed that, in the absence of unrest, the magma chamber is in lithostatic equilibrium with its host rock. This implies that the pressure in the magma chamber equals the host-

rock stresses normal to its surface (walls) at every point along the surface of the chamber. Since it is further assumed that the chamber is fluid (a free surface), it follows that at the surface of the chamber the principal stresses are all equal in magnitude and either parallel or perpendicular to the chamber. These stresses (more specifically, the stress vectors) must also, by definition, all be equal to the total fluid pressure (the lithostatic pressure) in the chamber at every point on its surface.

On the assumption of lithostatic state of stress, for a chamber in lithostatic equilibrium ('lithostatic conditions' [with] ' $\rho_r = \rho_m$ '), as is assumed in Fig. 5 of the EWS-model, there cannot be any difference between the 'across wall' (radial or normal), 'wall-parallel' (tangential or circumferential) stresses, and the vertical stress. Nor can there be any difference between any of these stresses at any point at the surface of the chamber and the total (lithostatic) pressure in the chamber. From these assumptions it also follows that the increase in total pressure in the chamber with depth is exactly balanced by the increase in the host-rock stresses on the chamber surface (or walls). Thus, from Eqs. (2) and (3) and the assumptions above it follows that the lithostatic stress in the host rock and the pressure in the chamber at any depth  $z$  is the same, namely  $\rho_r g z = \rho_m g z$ . This means that the stress below points A and B in Fig. (5a) is the same at any depth under consideration. Under these conditions, the effective stress (the stress giving rise to brittle deformation such as magma-chamber rupture and dyke injection) is zero, so that there is no tendency to large-scale brittle deformation of any kind. For static fluid pressure in a magma chamber, the mean stress is the hydrostatic pressure and we might thus also refer to the deviatoric stress, that is, the difference between the normal stress on a plane and the mean stress on that same plane, when discussing the conditions for brittle deformation around a magma chamber (Gudmundsson, 2011a). In volcanotectonics, the effective stress may be regarded as the excess pressure,  $p_e$  (Eqs. (10), (11)); which is the pressure that can give rise to magma-chamber rupture.

There is less-than-lithostatic fluid pressure in many porous hydrocarbon reservoirs. In fact, many have fluid pressures less than hydrostatic although some reach lithostatic pressures (Chilingar et al., 2002; Satter et al., 2008). But these are not totally fluid reservoirs, as is assumed in the EWS-model (and many other magma-chamber stress models), but rather porous and fractured rock bodies that are partially filled with fluids (oil, gas, and water). A totally fluid reservoir of any kind, such as the magma chambers discussed here, always seeks to be in a lithostatic equilibrium with the host rock at any point. If the reservoir is composed of pressure compartments (Fig. 15; see Section 7), so that the magma excess pressure may be higher in one part of the chamber than in other parts, the chamber would respond through expansion in high-pressure part and eventually, if the excess pressure reached the conditions of Eqs. (9)–(11), rupture and inject dykes or sheets. Thus, even if there are differences in the densities of the host rock and the magma, so that,  $\rho_r \neq \rho_m$ , and gradients in stress and excess pressure, the chamber would tend to reach an equilibrium geometry with the host rock. Effects of stress gradients on the geometry of fluid-filled crustal fractures are discussed by Secor and Pollard (1975) and Pollard (1976).

It follows from these considerations that there cannot be any extra 'wall-parallel component of the lithostatic stress' that resists magma-chamber rupture. If such a component existed, it would imply that the conditions  $\sigma_1 = \sigma_2 = \sigma_3$  (or  $\sigma_r = \sigma_\theta = \sigma_z$ ) were not satisfied, in direct contradiction with the definition of lithostatic state of stress. For the assumed lithostatic state of stress, the conclusions of the EWS-model as to the first point above are thus incorrect.

The second state of stress considered in the EWS-model is the well-known state of stress presented by Eqs. (6) and (8). It is often referred to as the condition of uniaxial strain. The application of this stress state to geological situations is briefly discussed in connection with Eq. (8) and in detail by Gudmundsson (2011a). The main

limitation, in the present context, is that this state of stress can never exist in the vicinity of a totally fluid magma chamber; normally, as soon as the stress difference  $\sigma_z - \sigma_\theta$  (in the EWS-model notation) reached the tensile strength of the rock at any point at the surface of the magma chamber, the chamber would rupture and a dyke or a sheet or a sill would be injected. The fluid overpressure of the magma-driven fracture (Eq. (12)) would lessen the stress difference so as to bring the state of stress close to lithostatic. This second state of stress is thus not appropriate when considering totally fluid magma chambers. That it is inappropriate is supported by the EWS-model results themselves which indicate that 'even when the magma pressure  $P=0$  [i.e., the excess pressure in the chamber is zero] the spherical cavity [the magma chamber] will fail when loaded by the weight of the enclosed magma alone, no other pressure component is required.' This would mean, of course, that no such magma chamber could form in the first place.

### 6.2.2. The second point

When a totally fluid magma chamber is subject to a 'pressure  $P$  which acts uniformly upon all the parts of reservoir wall', then if any part of the wall or surface has zero tensile strength there cannot be any significant excess pressure in the chamber at that point. Such a magma chamber could never give rise to any normal eruption since for an eruption to occur and be maintained over some significant time – eruption durations typically range from a few days to a few months (Simkin and Siebert, 2000) – there must be excess pressure in the chamber to drive out the magma (see Section 7 for the excess-pressure analysis). Also, the use of zero tensile strength neither fits with the other EWS-model estimates of magma-chamber excess pressures (and thus tensile strengths) of hundreds of megapascals, nor with measurements of in-situ tensile strengths. This brings us to the third point.

### 6.2.3. The third point

The third point suggests that magma chambers can tolerate magmatic excess pressures of hundreds of megapascals. In fact, the excess pressure needed for failure at great depths is apparently supposed to become close to 3-times the lithostatic stress. Laboratory and in-situ tensile-strength measurements have been carried out over many decades. The highest tensile strengths reported from laboratory measurements on small specimens are about 30 MPa (Carmichael, 1989; Hansen, 1998; Myrvang, 2001; Gudmundsson, 2011a and references therein). More appropriate for magma-chamber failure and dyke or sheet injection, however, are in-situ tensile strength measurements using hydraulic fracturing. These are made in a section of a borehole which is sealed off (by rubber packers). The fluid (usually water) pressure in this part is increased until the walls of the borehole fail, forming a fluid-driven extension fracture (a hydraulic fracture). The experiment is then repeated and the fluid-pressure difference between that at initial rupture (fracture formation) and new fluid injection into the new hydraulic fracture gives the in-situ tensile strength (Amadei and Stephansson, 1997; Myrvang, 2001; Zoback, 2007; Zang and Stephansson, 2010). The analogy with magma-chamber rupture and dyke injection is clear.

Worldwide results show that the in-situ tensile strengths of crustal rocks vary between 0.5 and 9 MPa, and are mostly 1–6 MPa (Haimson and Rummel, 1982; Schultz, 1995; Amadei and Stephansson, 1997; Zang and Stephansson, 2010). The strengths have been measured from the surface to depths of about 9 km. There is no known general increase in tensile strength of crustal rocks with depth. Neither are there any rocks known to tolerate tensile stresses of hundreds of megapascals before failure. The EWS-model conclusion that excess pressures at magma-chamber failure may be as high as hundreds of megapascals is thus without any support from direct measurements of tensile strengths of crustal rocks.

## 7. Chamber pressure variation during an eruption: effects of compartments

The stress condition for magma-chamber rupture can be reached in two basic ways (Gudmundsson, 1988, 2006; Folch and Marti, 1998): (i) through increasing the total pressure inside the chamber (for example, by adding magma to the chamber or through gas exsolution from its magma), and (ii) through external extension, such as in rift zones, where the divergent plate movements gradually reduce the minimum principal compressive stress  $\sigma_3$ . Both loadings increase the chamber excess pressure. The second type of loading (ii) generally favours the injection of vertical dykes, whereas the first type of loading (i) may sometimes favour dykes, and sometimes inclined sheets (and occasionally sills). Both loadings result in the increase of the magma-chamber excess pressure.

Once the excess pressure in a magma chamber reaches the conditions of rupture (Eqs. (9)–(11)), a magma-driven fracture (a dyke or an inclined sheet or, more rarely, a sill) is initiated. The stress conditions for the propagation of the fracture to the surface, resulting in an eruption or, alternatively, the arrest of the fracture at depth in the volcano (Fig. 1), have been discussed in many papers (e.g., Spence et al., 1987; Lister and Kerr, 1991; Clemens and Mawer, 1992; Petford et al., 1993; Rubin, 1995; Gudmundsson, 2002; Rivalta et al., 2005; Acocella and Neri, 2009; Geshi et al., 2010, 2012; Maccaferri et al., 2010, 2011; Moran et al., 2011; Taisne et al., 2011). I shall therefore not discuss the effect of magma-chamber stress fields on dyke propagation but rather focus on the excess-pressure changes in the chamber during the eruption.

Once the feeder-dyke has reached the surface, the volumetric flow rate of magma (assuming laminar flow) through the volcanic fissure  $Q$  is given by (e.g., Gudmundsson, 2011a):

$$Q = \frac{\Delta u^3 W}{12\mu_m} \left[ (\rho_r - \rho_m)g \sin\alpha - \frac{\partial p_e}{\partial L} \right] \quad (13)$$

where  $\Delta u$  is the opening or aperture of the feeder-dyke or volcanic fissure,  $W$  is the length or strike dimension of the feeder-dyke (the volcanic fissure) at the surface,  $\mu_m$  is the dynamic (absolute) viscosity and  $\rho_m$  the density of the magma (assumed constant),  $\rho_r$  is the average density of the crustal segment (including the volcano; Fig. 1) through which the dyke propagated to the surface,  $g$  is the acceleration due to gravity,  $\alpha$  is the dip of the feeder-dyke, and  $\partial p_e / \partial L$  is the vertical excess-pressure gradient in the direction of the magma flow, that is, in the direction of the dip dimension of the dyke  $L$ . Eq. (13) follows directly from the Navier–Stokes equation (Lamb, 1932; Milne-Thompson, 1996) and has been used in various forms for analysing magma transport to the surface (Wilson and Head, 1981; Lister and Kerr, 1991; Rubin, 1995; Gudmundsson and Brenner, 2005).

The total volume  $V$  that flows out of the poroelastic magma chamber through the feeder-dyke before the eruption comes to an end can be estimated as follows (Gudmundsson, 1987):

$$V = f p_e (\beta_p + \beta_m) V_c \quad (14)$$

where  $f$  is porosity (magma fraction) of the chamber,  $p_e$  is the magma excess pressure in the chamber before rupture and feeder-dyke formation,  $\beta_m$  is the magma compressibility and  $\beta_p$  the pore compressibility of the magma chamber, and  $V_c$  is the total volume of the chamber. Eq. (14) follows from poroelastic considerations (cf. Bear, 1972; Wang, 2000) and is widely applied in hydrogeology (Domenico and Schwartz, 1998; Deming, 2002). A non-porous (totally fluid) version of this equation has also been used for magma chambers (e.g., Machado, 1974; Blake, 1981). The flow out of the magma chamber through the feeder-dyke stops, and the eruption comes to an end, when the excess pressure is no longer able to keep the

dyke-fracture open at its contact with the chamber, that is, when  $p_e \rightarrow 0$ .

For dykes that do not reach the surface, that is, non-feeders, the fracture need not close when the dyke stops its propagation. When the dyke tip becomes arrested, the dyke propagation simply stops and the emplaced dyke solidifies and eventually cools down to the temperature of the host rock. In rare cases where the roof of an old magma chamber is exposed (Fig. 5), dykes may be seen connected with the magma chamber, particularly when the dyke magma is felsic and highly viscous. Most such dykes, particularly the comparatively thick ones, are presumably non-feeders. This follows because for the feeder-dykes, particularly basaltic ones, the contact with the magma chamber would normally effectively close at the end of the eruption.

Eqs. (13) and (14) can be combined to show theoretically how the excess pressure in the magma chamber during an eruption is likely to decrease. Here we consider only basaltic eruptions. The simplest way of showing this is to assume (1) that the volumetric flow rate over a given time  $t$  during the eruption can be expressed by some average value  $Qt$  and (2) that there is no density difference between the host rock and the magma, so that the term  $(\rho_r - \rho_m)gh$  in Eq. (13) is zero. This means that, for the present analysis, the magma transport up through the feeder dyke is entirely attributable to the excess-pressure gradient,  $\partial p_e / \partial L$ . These assumptions are only made so as to make the mathematical analysis more tractable; the results still capture the essential physics describing the excess-pressure changes in a magma chamber during an eruption.

During flow of magma out of the chamber through a dyke, the excess pressure  $p_c$  in the chamber at any instant is given by:

$$p_c = p_e - \psi \int_0^t Q dt \quad (15)$$

where  $p_e$  is the excess pressure at the time of magma-chamber rupture, that is, at  $t=0$ ,  $Q$  is the volumetric flow rate, and  $\psi$  is the reciprocal of the right-hand side of Eq. (14), namely:

$$\psi = [f(\beta_p + \beta_m)V_c]^{-1} = \frac{p_e}{V} \quad (16)$$

and has the units of  $\text{Pa m}^{-3}$ .

The volumetric flow rate  $Q$  as a function of time may be given as (Machado, 1974):

$$Q = Q_e - A \int_0^t Q dt \quad (17)$$

where  $Q_e$  is the initial volumetric flow rate and  $A$  is a constant that is related to Eqs. (13) and (14), in particular to the excess pressure and the compressibility and volume of the reservoir, as well as on the dimensions of the feeder dyke.

It can be shown that the solution to Eq. (17) is (Machado, 1974):

$$Q = Q_e e^{-At} \quad (18)$$

For an eruption, the volumetric flow rate is also referred to as the effusion rate. A similar equation was obtained by Wadge (1981). By analogy with Eq. (18), and using Eqs. (15) and (16), the excess pressure in the magma chamber after time  $t$  as a function of magma flow out of the chamber (feeder-dyke plus eruptive materials) during that time interval is (cf. Woods and Huppert, 2003):

$$p_c = p_e e^{-(Qt/V)} \quad (19)$$

where all the symbols are as defined above and the exponent has the units of volume divided by volume and is therefore dimensionless.

Eqs. (18) and (19) show that, for the given boundary conditions, the volumetric flow rate through the feeder dyke (eruptive fissure) and the magmatic excess pressure in the chamber should decrease exponentially during the eruption. These equations have the same

form as the well-known equation for the relaxation of viscoelastic and poroelastic bodies (e.g., Williams, 1980; Christensen, 1982; Wang, 2000; Yu, 2000). For example, for Eq. (19) the only differences are that for a viscoelastic Maxwell body, Young's modulus is substituted for the volumetric flow rate  $Q$  and the dynamic viscosity of the viscous part of the Maxwell body is substituted for the erupted (and intruded) volume  $V$  (Williams, 1980). This analogy is as expected because the excess-pressure decrease in the chamber is formally analogous to the relaxation or decrease of stress in a viscoelastic body.

That the volumetric flow rates falls roughly exponentially during an eruption is commonly observed (Machado, 1974; Wadge, 1981; Thordarson and Self, 1993; Thordarson and Larsen, 2007). Similarly, roughly exponential decrease in excess pressure during an eruption is probably a common feature in magma chambers. However, these conclusions rest not only on the assumptions given above, but also on the assumptions that (1) the contribution of the exsolved volatiles and (2) replenishment (inflow of new magma into the chamber) have negligible effects on the excess pressure evolution in the chamber during the eruption. The contribution of exsolved volatiles to the excess pressure in the chamber has been discussed in detail by many authors (e.g., Tait and Jaupart, 1989; Woods and Huppert, 2003), but is likely to be minimal for typical basaltic eruptions. The effects of replenishment on the excess-pressure evolution in the chamber have also been considered by others (e.g., Woods and Huppert, 2003). However, for most eruptions, the volumetric flow rate out of the chamber during an eruption is many times larger than the rate of flow into the chamber (from a deeper source reservoir), so that this effect on the excess pressure variation is commonly minimal (Stasiuk et al., 1993; Gudmundsson, 2006).

From Eqs. (13), (14), (17), and (18), the volumetric flow rate or effusion rate depends on the variation in the excess pressure in the chamber, but also on other factors. From Eq. (13), these factors include the length of the feeder-dyke/volcanic fissure, the dynamic viscosity of the magma, the density difference between the magma and the host rock, the dip of the feeder-dyke, and the opening/aperture of the feeder-dyke/volcanic fissure at the surface. For a basaltic magma of a given composition and viscosity, even if the length of the fissure may (and often does) change during the eruption, the main effect on the volumetric flow rate would still be the variation in aperture. This is because the volumetric flow rate for laminar flow depends on the aperture in the third power – referred to as the cubic law – so that small changes in the size of the aperture may have large effects on the volumetric flow rate (e.g., Wilson and Head, 1981; Stasiuk et al., 1993; Gudmundsson and Brenner, 2005).

Although many effusion rates show a gradual decline from a peak early in the eruption until it comes to an end (Machado, 1974; Wadge, 1981; Stasiuk et al., 1993; Thordarson and Self, 1993; Thordarson and Larsen, 2007), there are commonly irregularities in the volumetric flow rates. For example, the volumetric flow may increase late in the eruption (Gudmundsson and Brenner, 2005), and the composition of the magma may change. The latter is very common in eruptions in stratovolcanoes and calderas where the initial magma is the most evolved and becomes less so (more primitive or mafic) during the course of the eruption.

Variation in flow rates may, as indicated above, be partly related to changes in feeder-dyke/fissure apertures as well as to density (hence buoyancy) changes of the magma during the course of the eruption. Changes both in flow rates as well as in composition, however, are likely to be commonly related to processes inside the associated magma chamber. In particular, some changes in volumetric flow rate and composition may be related to magma-chamber compartments and their interactions.

As indicated above, compartments are well known in petroleum reservoirs (Economides and Nolte, 2000; Deming, 2002; Satter et al., 2008) but have received hardly any attention in volcanology. It is

well known, however, that nearby volcanic fissures in the same volcano and, given their location, from the same magma chamber, separated by geologically short periods of time (tens or hundreds of years), may produce eruptions of widely different duration and erupt materials with a widely different composition. This indicates that there are nearby parts or volumes inside a magma chamber that have minimal interaction (exchange of materials), that is, form different compartments within a single magma chamber. These are commonly referred to as pressure compartments for hydrocarbon reservoirs (Deming, 2002). They are generally explained in terms of structural constraints or boundaries, including faults and pressure seals, that to a large extent isolate one part of the reservoir from its other parts.

An example of such a division of a magma chamber into compartments is through faulting, particularly following nested caldera (or graben) formation (Fig. 15). Here the magmas at different elevations in the chamber are unlikely to mix laterally because the faults are barriers to the lateral fluid flow. For a density stratified magma chamber, the same magmas are unlikely to mix vertically. It follows that in the schematic scenario illustrated in Fig. 15 the chamber may be divided into compartments, such as those indicated by the numbers 1–5. Before and shortly after fault formation, the magmas in compartments 1 and 5 may have had very similar compositions, but subsequently they could evolve differently (through fractionation and anatexis and stoping) so as to become quite different magmas. The same applies to the magmas in compartments 2 and 4. Even if the faults were ring faults, lateral flow is unlikely along large parts of the faults (so as to allow mixing between compartments, say, 90° apart or 180° apart). This follows because lateral flow along fractures tends to be perpendicular to the minimum principal compressive stress,  $\sigma_3$ , and thus occupy that part of the ring fault that does not deviate much from being roughly perpendicular to  $\sigma_3$ .

While faults and other ‘seals’ may contribute to the compartmentalisation of magma chambers, perhaps a more common reason for compartments is the way magma chambers form. It is now recognised that most magma chambers form through many magma injections (Figs. 5, 8). For the fossil chamber of Slaufudalur (Fig. 5) the contacts between the sills are still seen, so that the sills may have acted as compartments with a minimal exchange of materials between them.

There are, however, other ways for magma chambers to form gradually over long periods of time. For example, the Vesturhorn Pluton in

Southeast Iceland, a fossil magma chamber, is thought to be composed of at least 70 smaller intrusions (Fig. 16; Roobol, 1974). With an exposed area of around 20 km<sup>2</sup>, Vesturhorn, of late Tertiary age, is the largest pluton in Iceland and is located in a 900-m-thick pile of basaltic lava flows with a regional dip of 7° NW. At the contacts with the pluton, however, the dips of the lava flows increase to as much as 30°, mostly away from the pluton, indicating, again, that many magma chambers/plutons generate space for themselves partly through forceful intrusion, primarily by bending the layers above (and below). Part of the roof is preserved (Fig. 16); it consists of flat-lying basaltic lava flows. Based on field mapping, Roobol (1974) proposed that the exposed part of the pluton is composed of at least 70 different intrusions. However, the main parts of the pluton are a ring complex, primarily of various types of gabbros and granophyres, an eastern mafic complex, and several epigranite bodies.

Similarly, the Austurhorn Pluton in Southeast Iceland is a large fossil magma chamber composed of many intrusions (Fig. 17; Furman et al., 1992; Thorarinsson and Tegner, 2009). For example, its main gabbro body (Fig. 17) is composed of at least 8 major units (Thorarinsson and Tegner, 2009). These units show clear evidence of having (i) received new magma injections (replenishment), followed by periods of normal crystal and liquid fractionation, (ii) compositional variation with stratigraphic elevation within the exposed part of the chamber, and (iii) acted as a magma chamber for a major stratovolcano. Within the Hvalnessfjall gabbro, the main melt lens at any particular time may have been quite thin; Thorarinsson and Tegner (2009) estimate it at 200–300 m.

Most magma chambers are not totally molten (except perhaps small sill-like chambers soon after their initiation), but rather a mixture of melt and a crystal mush (e.g., Marsh, 1989; Sinton and Detrick, 1992; Marsh, 2000; Dobran, 2001; Parfitt and Wilson, 2008). Various estimates have been made of the actual amount of melt in a body identified as a magma chamber, but this amount is surely going to vary a lot during the lifetime of the chamber. One geophysical estimate for a basaltic magma chamber beneath the Juan de Fuca Ridge (just offshore the west coast of North America) indicates that the actual melt in the chamber, located at a depth of about 2–6 km below the ocean floor and with an estimated volume of 250 km<sup>3</sup>, is only 2–8% of the total chamber volume (West et al., 2001).

Compartments in magma chambers exchange energy (heat) but commonly little if any matter (over long periods of time) and are thus effectively closed thermodynamic systems. This implies that

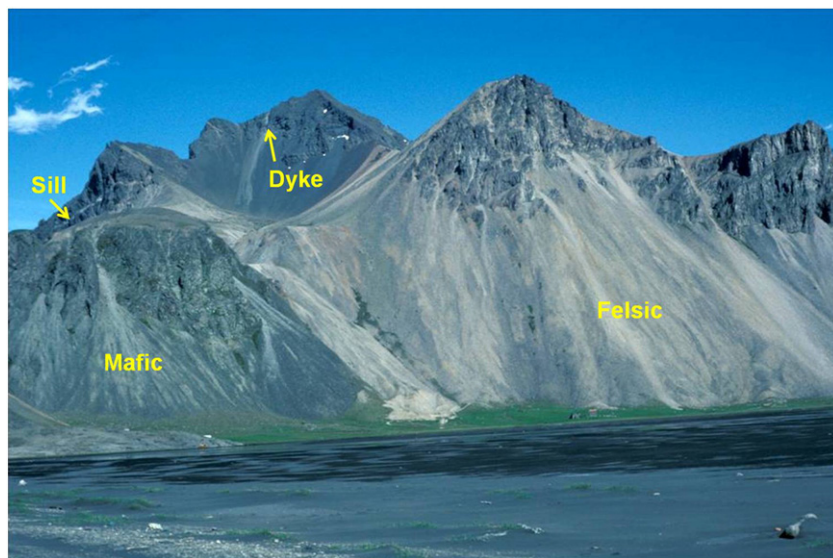


**Fig. 16.** Part of the fossil magma chamber Vesturhorn in Southeast Iceland (its maximum height is 889 m). View northwest, the pluton is composed partly of felsic (granophyre) and partly of mafic (gabbro) bodies (some are indicated). Also indicated are a dyke and a sill dissecting the roof. The pluton has an exposed area of some 20 km<sup>2</sup>, is composed of more than 70 individual intrusive bodies of various sizes (Roobol, 1974), and is the largest pluton in Iceland.



**Fig. 17.** Part of the fossil magma chamber Austurhorn in Southeast Iceland (its height as seen here is 606 m). View northwest, the pluton is composed of many smaller intrusions, of mafic and felsic composition (cf. Furman et al., 1992; Thorarinnsson and Tegner, 2009).

during eruptions the composition of eruptive materials issued from nearby fissures fed by the same magma chamber may differ considerably (Fig. 18). This applies, in particular, to small eruptions each of which tends to draw its magma entirely from a single compartment (numbered 1–5 in Fig. 18). For larger eruptions, the magma is gradually drawn from deeper parts of the compartments (numbered 1a–3a in Fig. 18), whereby drawdown may lower the hydraulic potential so as to allow magma to migrate into the compartment from nearby compartments; for example from 2a and/or 3a to 1a during eruptions from compartment number 1 (Fig. 18).

There are thus likely to be some threshold values as regards lowering of the hydraulic potential (or pressure) in a compartment for magma from nearby compartments to start to migrate towards the erupting compartment. The melt migration through the crystal mush follows Darcy's law of fluid flow in porous media (Bear, 1972; McKenzie, 1984; Gudmundsson, 1987; Dobran, 2001; Bachmann and Bergantz, 2004). The flow is driven by the hydraulic gradient or, in the case of purely horizontal flow, by the pressure gradient. The flow rate depends on the permeability and porosity of the crystal mush, as well as on the viscosity and density of the melt and the cross-sectional areas of the channels through which it flows.

When magma from an adjacent compartment is able to flow into the erupting compartment, the excess pressure necessary to continue the eruption may be maintained for a longer time (Eqs. 15–19). It follows that the duration of the eruption may be longer than if only the original compartment provided all the magma. Furthermore, the composition of the erupted magma is likely to change during the course of the eruption, as the new melt comes in from the adjacent compartment(s). If new melt is injected from a deeper source during the eruption, it is most likely to be of high density and may pond on the floor of the chamber (Fig. 18).

## 8. Discussion

A magma chamber is normally a necessary condition for the formation of a major, polygenetic volcano. To improve our understanding of the long-term behaviour and activities of stratovolcanoes, collapse calderas, and basaltic edifices, we must know the mechanical, and especially the stress, conditions for the initiation and evolution of the associated magma chambers. In particular, we need to understand the condition for the growth of a magma chamber from its nucleus, that is, the initial intrusion, to its quasi-stable geometric

form. Most importantly, the local stresses around the chamber must be known if we are to forecast successfully magma-chamber rupture and dyke/sheet injection. When the conditions for chamber rupture are met, reliable stress models are needed to assess the likelihood that the resulting dyke/sheet will reach the surface and supply magma to an eruption. Once an eruption has started, its duration depends largely on the associated excess-pressure changes in the chamber.

This paper provides a review and analysis of many current ideas and models, and presents some new ideas, as to the formation and geometric evolution of magma chambers. Field data and theoretical considerations indicate that most magma chambers are formed through many magma injections; a few, presumably mostly small sill-like chambers, are formed in single magma injections. These

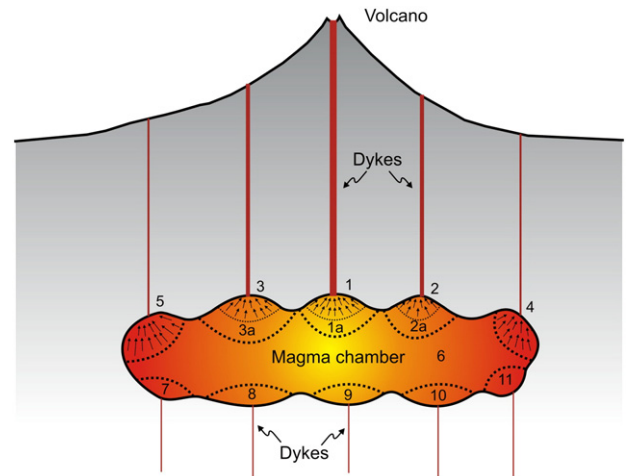


**Fig. 18.** Schematic illustration of possible compartments in a magma chamber. Compartments 1–5 are composed of comparatively low-density magmas, whereas those number 7–11 are of high-density magmas (and, in this illustration, related to injection of primitive (basaltic) magmas from a deeper magma source). During typical small eruptions from compartments 1–5, magma is derived only from the compartment with which the feeder dyke is connected. For larger eruptions, magma is drawn from deeper parts of the specific compartments (indicated by the numbers 1a, 2a, and 3a), and the associated lowering of the hydraulic potential may eventually result in magma being driven into that compartment from one or more adjacent ones (for example, driven from compartment 2 to compartment 1 during a comparatively large eruption from compartment 1).

views are elaborated in many recent papers and special issues, such as by Menand et al. (2011). Examples of magma chambers generated in many injections are given in Figs. 5, 8, 10, 16, and 17. Field data and theoretical considerations also indicate that many magma chambers initiate from multiple sill injections of various shapes (Figs. 5, 8), whereas other multiple sills or sill clusters failed to evolve into chambers (Figs. 3, 4). These observations relate to the modelling of the state of stress around magma chambers.

While most analytical and numerical models on magma-chamber stress field use the same basic assumptions as to how to model a fluid-filled chamber (e.g., McTigue, 1987; Tait and Jaupart, 1989; Gudmundsson, 2002), a widely different approach has recently been used by Grosfils and co-workers (Grosfils, 2007; the EWS-model) who suggest that the standard approach results in several incorrect results. Among the supposed-to-be incorrect results are (a) the presumed low magmatic excess pressure needed for magma-chamber rupture and dyke injection, and (b) the presumed depth-independence of the conditions for magma-chamber rupture and dyke injection.

The theoretical and observational considerations in the present paper, however, indicate that the main differences between the previous models and the stress-predictions of the EWS-model rest on some misunderstandings in the latter. In particular, for many scenarios the EWS-model assumes a lithostatic state of stress, and a chamber in lithostatic equilibrium with the host rock. It also assumes magma density equal to the host-rock density and (in some cases) zero tensile strength of the host rock. These assumptions imply that there cannot be any extra wall-parallel stress, related to lithostatic stress, that resists magma-chamber (wall) rupture and dyke or sheet injection. The assumptions also imply that a chamber cannot contain magma with excess pressures of as much as several hundred megapascals. Furthermore, neither of these EWS-model predictions (extra wall-parallel stress; excess pressures reaching hundreds of megapascals) is supported by direct measurements in drill-holes—measurements that reach to crustal depths of as much as 9 km.

While considerable progress has been made in recent decades in understanding the formation, geometry, and crustal stress fields of magma chambers, as well as the constraints on their excess pressures, comparatively little work has been done on excess-pressure changes during eruptions and the possibility of pressure compartments. Pressure compartments are common in many fluid reservoirs in the crust, particularly in hydrocarbon reservoirs, and are being modelled, but magma-chamber pressure compartments have not received much attention. The present paper outlines some possible compartment scenarios (Figs. 15, 18) and show examples of fossil magma chambers where such compartments are likely to have evolved over certain periods of time (Figs. 10, 16, 17).

Various aspects of the chemical/petrological evolution of magma chambers are comparatively well understood, but there is a need for much more sophisticated models and a deeper understanding of the physics and tectonic evolution of magma chambers. In particular, we need to learn how to model the pressure changes in double magma chambers, that is, chambers that receive magma from a deeper source (are replenished) during an on-going eruption. While some general models exist on various aspect of this problem (e.g., Woods and Huppert, 2003; Gudmundsson, 2006), more detailed work is needed. In particular, the potential effects of compartments and double-magma chambers on the excess-pressure distribution in the magma chamber need to be studied since these affect the length of (and compositional changes during) the associated volcanic eruptions.

Replenishment and compartments also relate to the question of magma-chamber lifetimes. For how long, and in which way, is a magma chamber maintained as an active source for a polygenetic volcano? Many volcanoes are active for hundreds of thousands of years and some for millions of years. Frequent replenishment of the magma chamber is necessary so as to maintain its function as a source for hundreds of thousands of years (Huppert and Sparks, 1980;

Sparks et al., 1984; Jaupart and Tait, 1995; Spera and Bohrsen, 2001; Annen and Sparks, 2002; Walker et al., 2007), and these replenishments affect the internal structure of the chamber and how it develops and responds to local stress fields.

## 9. Conclusions

Some of the main conclusions of the paper may be summarised as follows:

- (1) Most magma chambers form and grow through repeated injections of magma. Many chambers develop from sills, and some retain their sill-like geometries throughout their lifetimes.
- (2) While active, a magma chamber acts as a sink for magma (receives magma) from a deeper source (or sources), here referred to as a reservoir, and as a source (ejects or injects magma) for an associated volcano. Some magma chambers, particularly small-sill like chambers during their early stages of evolution, may be totally molten, but most magma chambers are partially molten, that is, porous bodies.
- (3) A magma chamber that is originally with very irregular boundaries is thermally (and mechanically) unstable. The host-rock jogs that project into the magma tend to melt, and the magma-filled notches that project into the host rock tend to solidify. It follows that the long-term equilibrium geometries of magma chambers tend towards comparatively smooth (commonly ellipsoidal) geometries.
- (4) When modelling magma chamber stress fields, rupture, dyke injection and association eruptions, three pressure concepts are needed and must be distinguished. These are excess pressure ( $p_e$ ), overpressure or driving pressure ( $p_o$ ), and total pressure ( $p_t$ ). Excess pressure is normally similar to the in-situ tensile strength of the host rock, that is, a few megapascals. Overpressure applies primarily to propagating sheet-like intrusions, such as dykes, and is the magmatic excess pressure plus the pressure related to the density difference between magma and the host rock through which the dyke is propagating. Depending on this density difference (buoyancy effects), overpressure can reach tens of megapascals. Total pressure is the excess pressure/overpressure plus the lithostatic pressure/stress at the point of observation in the dyke or magma chamber.
- (5) During an eruption, the excess pressure normally decreases in the source chamber until it becomes close to zero, at which time the dyke-fracture normally closes and the eruption comes to an end. On the assumption of negligible replenishment and no contribution from gas exsolution to the excess pressure during the eruption (both assumptions may be valid for typical basaltic eruptions of short duration), the excess pressure decreases exponentially until the dyke closes at its junction with the chamber.
- (6) Standard models of magma-chamber stress fields use excess pressure as the only loading. In the absence of unrest periods, most magma chambers should be in a lithostatic equilibrium with their host rocks. Lithostatic equilibrium implies lithostatic state of stress so that all the principal stresses must be equal in magnitude and either parallel or perpendicular to the chamber, that is,  $\sigma_1 = \sigma_2 = \sigma_3$ . And these stresses must, by definition, all be equal to the total fluid pressure (the lithostatic pressure) in the chamber at every point at its surface.
- (7) The standard models suggest as follows. The magmatic excess pressure before chamber rupture and dyke (or sheet or sill) injection from the chamber is roughly equal to the in-situ tensile strength of the host rock, or between about 0.5 and 9 MPa and most commonly between 1 and 6 MPa. (b) The stress condition for magma-chamber rupture can be reached in two basic

ways: (i) through increasing the total pressure inside the chamber (for example, by adding magma to the chamber or through gas exsolution from its magma), and (ii) through external extension, such as in rift zones, where the divergent plate movements gradually reduce the minimum principal compressive stress  $\sigma_3$ . Both loading conditions increase the chamber excess pressure. The second type of loading (ii) generally favours the injection of vertical dykes, whereas the first type of loading (i) sometimes favours vertical dykes, and sometimes inclined sheets (and occasionally sills).

- (8) The local stress field around a magma chamber depends, in addition to the general loading conditions, on the magma-chamber shape, its depth below the earth's surface, and the mechanical properties, in particular the mechanical layering, of the host rock. This is demonstrated by recent analytical and numerical models showing the effects of layering on the local stresses and surface deformation in volcanoes during excess-pressure changes in magma chambers.
- (9) Some recent magma-chamber modelling takes a very divergent view as to the loading conditions and, in particular, the effects of gravity on the local stresses at the chamber boundary. In particular, these models claim that (a) there are extra wall-parallel components of the lithostatic stress that act against magma-chamber rupture, (b) magmatic excess pressures before chamber rupture can be so high as several hundred megapascals, and (c) the excess pressure that the chamber can tolerate without rupture increases with the chamber depth. A detailed study of these models indicates that some of their conclusions rest on misunderstandings as to the implications of a lithostatic state of stress. Furthermore, the predicted stress and pressure variations are not supported by worldwide measurements of crustal stresses and in-situ tensile strengths in drill holes, extending to crustal depths of 9 km. None of these measurements indicate any extra wall-parallel stresses nor do they show any evidence of a large depth-related increase in in-situ tensile strengths (roughly equal to the excess pressures at rupture) which nowhere reach measured values in excess of about ten megapascals.
- (10) While there has been a significant progress in our understanding of magma-chamber formation, geometry, and stress fields in the past decades, as well as in understanding their chemical and petrological evolution, there has been much less progress as to the internal structural development and properties of chambers. In particular, potential pressure compartments, some of which may differ widely in their mechanical (and chemical) properties, have received little attention in volcanology. Understanding such compartments requires the combination of analysis of fossil magma chambers (plutons), geophysical studies of active magma chambers, and analytical and numerical modelling as to the potential effects of compartments on the transport of heat and melt between the different parts of the chamber prior to and during volcanic eruptions.

## Acknowledgements

I thank the Editor Lionel Wilson and the Managing Editor Timothy Horscroft for inviting me to write this review of our knowledge of the tectonic aspects of magma chambers with a focus on divergent views as to the associated stress fields. I also thank Maurizio Bonafede and an anonymous reviewer for very helpful comments.

## References

- Acocella, V., 2007. Understanding caldera structure and development: and overview of analogue models compared to natural calderas. *Earth-Science Reviews* 85, 125–160.

- Acocella, V., Neri, M., 2009. Dike propagation in volcanic edifices: overview and possible development. *Tectonophysics* 471, 67–77.
- Amadei, B., Stephansson, O., 1997. *Rock Stress and its Measurement*. Chapman and Hall, London.
- Anderson, E.M., 1936. The dynamics of formation of cone sheets, ring dykes and cauldron subsidences. *Proceedings of the Royal Society of Edinburgh* 56, 128–163.
- Andrew, R.E.B., Gudmundsson, A., 2008. Volcanoes as elastic inclusions: their effects on the propagation of dykes, volcanic fissures, and volcanic zones in Iceland. *Journal of Volcanology and Geothermal Research* 177, 1045–1055.
- Annen, C., Sparks, R.S.J., 2002. Effects of repetitive emplacement of basaltic intrusions on the thermal evolution and melt generation in the crust. *Earth and Planetary Science Letters* 203, 937–955.
- Bachmann, O., Bergantz, G.W., 2004. On the origin of crystal-poor rhyolites: extracted from batholithic crystal mushes. *Journal of Petrology* 45, 1565–1582.
- Balme, M.R., Rocchi, V., Jones, C., Sammonds, P.R., Meredith, P.G., Boon, S., 2004. Fracture toughness measurements on igneous rocks using a high-pressure, high-temperature rock fracture mechanics cell. *Journal of Volcanology and Geothermal Research* 132, 159–172.
- Bear, J., 1972. *Dynamics of Fluids in Porous Media*. Elsevier, Amsterdam.
- Bell, F.G., 2000. *Engineering Properties of Soils and Rocks*, 4th ed. Blackwell, Oxford.
- Beswick, A.E., 1965. A study of the Slaufudalur Granophyre Intrusion, South-East Iceland. PhD Thesis, Imperial College, London.
- Blake, D.H., 1966. The net-veined complex of the Austurhorn intrusion, southeastern Iceland. *Journal of Geology* 74, 891–907.
- Blake, S., 1981. Volcanism and the dynamics of open magma chambers. *Nature* 289, 783–785.
- Bonaccorso, A., Cianetti, S., Giunchi, C., Trasatti, E., Bonafede, M., Boschi, E., 2005. Analytical and 3D numerical modeling of Mt. Etna (Italy) volcano inflation. *Geophysical Journal International* 163, 852–862.
- Bonafede, M., Ferrari, C., 2009. Analytical models of deformation and residual gravity changes due to a Mogi source in a viscoelastic medium. *Tectonophysics* 471, 4–13.
- Bonafede, M., Dragoni, M., Quarenì, F., 1986. Displacement and stress fields produced by a centre of dilation and by a pressure source in a viscoelastic half-space: application to the study of ground deformation and seismic activity at Campi Flegrei, Italy. *Geophysical Journal of the Royal Astronomical Society* 87, 455–485.
- Boresi, A.P., Sidebottom, O.M., 1985. *Advanced Mechanics of Materials*, 4th ed. Wiley, New York.
- Bradley, J., 1965. Intrusion of major dolerite sills. *Transactions of the Royal Society of New Zealand* 3, 27–55.
- Bunger, A.P., Cruden, A.R., 2011. Modeling the growth of laccoliths and large mafic sills: role of magma body forces. *Journal of Geophysical Research* 116, B02203. <http://dx.doi.org/10.1029/2010JB007648>.
- Canales, J.P., Nedimovic, M.R., Kent, G.M., Carbotte, S.M., Detrick, R.S., 2009. Seismic reflection images of a near-axis melt sill within the lower crust at the Juan de Fuca ridge. *Nature* 460, 89–93.
- Cargill, H.K., Hawkes, L., Ledebøer, J.A., 1928. The major intrusions of south-eastern Iceland. *Quarterly Journal of the Geological Society of London* 84, 505–539.
- Carmichael, R.S., 1989. *Practical Handbook of Physical Properties of Rocks and Minerals*. CRC Press, Boca Raton, Boston.
- Chevallier, L., Woodford, A., 1999. Morpho-tectonics and mechanism of emplacement of the dolerite rings and sills of the western Karoo, South Africa. *South African Journal of Geology* 102, 43–54.
- Chilingar, G.V., Serebryakov, V.A., Robertson, J.O., 2002. *Origin and Prediction of Abnormal Formation Pressures*. Elsevier, Amsterdam.
- Christensen, R.M., 1982. *Theory of Viscoelasticity*. Dover, New York.
- Clemens, J.D., Mawer, C.K., 1992. Granitic magma transport by fracture propagation. *Tectonophysics* 204, 339–360.
- Daneshy, A.A., 1978. Hydraulic fracture propagation in layered formations. *AIME Society of Petroleum Engineers Journal* 33–41.
- Davis, P.M., 1986. Surface deformation due to inflation of an arbitrarily oriented triaxial ellipsoidal cavity in an elastic half space, with reference to Kilauea volcano, Hawaii. *Journal of Geophysical Research* 91, 7429–7438.
- De Natale, G., Pingue, F., 1993. Ground deformation in collapsed calderas structures. *Journal of Volcanology and Geothermal Research* 57, 19–38.
- Deming, D., 2002. *Introduction to Hydrogeology*. McGraw-Hill, New York.
- Dobran, F., 2001. *Volcanic Processes*. Kluwer, New York.
- Domenico, P.A., Schwartz, F.W., 1998. *Physical and Chemical Hydrogeology*, 2nd ed. Wiley, New York.
- Dzurisin, D., 2006. *Volcano Deformation: New Geodetic Monitoring Techniques*. Springer, Berlin.
- Economides, M.J., Nolte, K.G. (Eds.), 2000. *Reservoir Stimulation*. Wiley, New York.
- Fjeldskaar, W., Helset, H.M., Johansen, H., Grunnaleite, I., Horstad, I., 2008. Thermal modelling of magmatic intrusions in the Gjallar Ridge, Norwegian Sea: implications for vitrinite reflectance and hydrocarbon maturation. *Basin Research* 20, 143–159.
- Folch, A., Marti, J., 1998. The generation of overpressure in felsic magma chambers. *Earth and Planetary Science Letters* 163, 301–314.
- Folch, A., Fernandez, J., Rundle, J.B., Marti, J., 2000. Ground deformation in a viscoelastic medium composed of a layer overlying a half-space: a comparison between point and extended sources. *Geophysical Journal International* 140, 37–50.
- Francis, E.H., 1982. Magma and sediment—I. Emplacement mechanism of late Carboniferous tholeiite sills in northern Britain. *Journal of the Geological Society of London* 139, 1–20.
- Frank, F., 2003. *Handbook of the 1350 active volcanoes of the world*. Otto Verlag, Thun, Switzerland. 192 pp. (in German).
- Furman, T., Meyer, P.S., Frey, F., 1992. Evolution of Icelandic central volcanoes: evidence from the Austurhorn intrusion, southeastern Iceland. *Bulletin of Volcanology* 55, 45–62.

- Fyfe, W.S., Price, N.J., Thompson, A.B., 1978. Fluids in the Earth's Crust. Elsevier, Amsterdam.
- Geshi, N., Kusumoto, S., Gudmundsson, A., 2010. Geometric difference between non-feeders and feeder dikes. *Geology* 38, 195–198.
- Geshi, N., Kusumoto, S., Gudmundsson, A., 2012. Effects of mechanical layering of host rocks on dike growth and arrest. *Journal of Volcanology and Geothermal Research* 223, 74–82.
- Geyer, A., Marti, J., 2008. The new worldwide collapse caldera database (CCDB): a tool for studying and understanding caldera processes. *Journal of Volcanology and Geothermal Research* 175, 334–354.
- Geyer, A., Marti, J., 2009. Stress fields controlling the formation of nested and overlapping calderas: implications for the understanding of caldera unrest. *Journal of Volcanology and Geothermal Research* 181, 185–195.
- Geyer, A., Folch, A., Marti, J., 2006. Relationship between caldera collapse and magma chamber withdrawal: an experimental approach. *Journal of Volcanology and Geothermal Research* 157, 375–386.
- Gray, T.G.F., 1992. *Handbook of Crack Opening Data*. Abingdon, Cambridge.
- Gretener, P.E., 1969. On the mechanics of the intrusion of sills. *Canadian Journal of Earth Sciences* 6, 1415–1419.
- Grosfils, E.B., 2007. Magma reservoir failure on the terrestrial planets: assessing the importance of gravitational loading in simple elastic models. *Journal of Volcanology and Geothermal Research* 166, 47–75.
- Gudmundsson, A., 1987. Formation and mechanics of magma reservoirs in Iceland. *Geophysical Journal of the Royal Astronomical Society of London* 91, 27–41.
- Gudmundsson, A., 1988. Effect of tensile stress concentration around magma chambers on intrusion and extrusion frequencies. *Journal of Volcanology and Geothermal Research* 35, 179–194.
- Gudmundsson, A., 1990. Emplacement of dikes, sills and crustal magma chambers at divergent plate boundaries. *Tectonophysics* 176, 257–275.
- Gudmundsson, A., 2002. Emplacement and arrest of sheets and dykes in central volcanoes. *Journal of Volcanology and Geothermal Research* 116, 279–298.
- Gudmundsson, A., 2006. How local stresses control magma-chamber ruptures, dyke injections, and eruptions in composite volcanoes. *Earth-Science Reviews* 79, 1–31.
- Gudmundsson, A., 2011a. *Rock Fractures in Geological Processes*. Cambridge University Press, Cambridge. 592 pp.
- Gudmundsson, A., 2011b. Deflection of dykes into sills at discontinuities and magma-chamber formation. *Tectonophysics* 500, 50–64.
- Gudmundsson, A., Brenner, S.L., 2005. On the conditions of sheet injections and eruptions in stratovolcanoes. *Bulletin of Volcanology* 67, 768–782.
- Haimson, B.C., Rummel, F., 1982. Hydrofracturing stress measurements in the Iceland research drilling project drill hole at Reydarfjörður, Iceland. *Journal of Geophysical Research* 87, 6631–6649.
- Hansen, S.E., 1998. Mechanical properties of rocks. Report STF22 A98034. Trondheim, Sintef. (in Norwegian).
- Hansen, D.M., Cartwright, J., 2006. The three-dimensional geometry and growth of forced folds above saucer-shaped igneous sills. *Journal of Structural Geology* 28, 1520–1535.
- Hawkes, L., Hawkes, H.K., 1933. The Sandfell laccolith and "dome of elevation". *Quarterly Journal of the Geological Society of London* 89, 379–400.
- Holmes, A., 1965. *Principles of Physical Geology*, 2nd ed. Nelson, London.
- Hubbert, M.K., Willis, D.G., 1957. Mechanics of hydraulic fracturing. *Transactions of the American Institute of Mining, Metallurgical and Petroleum Engineers* 210, 153–168.
- Huppert, H.E., Sparks, R.S.J., 1980. The fluid-dynamics of a basaltic magma chamber replenished by influx of hot, dense ultrabasic magma. *Contributions to Mineralogy and Petrology* 75, 279–289.
- Hurwitz, D.M., Long, S.M., Grosfils, E.B., 2009. The characteristics of magma reservoir failure beneath a volcanic edifice. *Journal of Volcanology and Geothermal Research* 188, 379–394.
- Jaeger, J.C., 1961. The cooling of irregularly shaped igneous bodies. *American Journal of Science* 259, 721–734.
- Jaeger, J.C., 1964. Thermal effects of intrusions. *Reviews of Geophysics* 2, 443–466.
- Jaeger, J.C., Cook, N.G.W., Zimmerman, R., 2007. *Fundamentals of Rock Mechanics*, 3rd ed. Wiley, London.
- Jaupart, C., Tait, S., 1995. Dynamics of differentiation in magma reservoirs. *Journal of Geophysical Research* 100, 17,615–17,636.
- Kavanagh, J.L., Menand, T., Sparks, R.S.J., 2006. An experimental investigation of sill formation and propagation in layered elastic media. *Earth and Planetary Science Letters* 245, 799–813.
- Kilburn, C.J., 2000. Lava flows and flow fields. In: Sigurdsson, H. (Ed.), *Encyclopedia of Volcanoes*. Academic Press, New York, pp. 291–305.
- Kilburn, C.J., McGuire, B., 2001. *Italian Volcanoes*. Terra Publishing, Harpenden (UK).
- Kusumoto, S., Gudmundsson, A., 2009. Magma-chamber volume changes associated with ring-fault initiation using a finite-sphere model: application to the Aira caldera, Japan. *Tectonophysics* 471, 58–66.
- Kusumoto, S., Takemura, K., 2005. Caldera geometry determined from by the depth of the magma chamber. *Earth Planets Space* 57, 17–20.
- Lamb, H., 1932. *Hydrodynamics*, 6th ed. Cambridge University Press, Cambridge.
- Lister, J.R., Kerr, R.C., 1991. Fluid-mechanical models of crack propagation and their application to magma transport in dykes. *Journal of Geophysical Research* 96, 10,049–10,077.
- Long, S.M., Grosfils, E.B., 2009. Modeling the effect of layered volcanic material on magma reservoir failure and associated deformation, with application to Long Valley Caldera, California. *Journal of Volcanology and Geothermal Research* 186, 349–360.
- Maaloe, S., Scheie, A., 1982. The permeability controlled accumulation of primary magma. *Contributions to Mineralogy and Petrology* 81, 350–357.
- Maccaferri, F., Bonafede, M., Rivalta, E., 2010. A numerical model of dyke propagation in layered elastic media. *Geophysical Journal International* 180, 1107–1123.
- Maccaferri, F., Bonafede, M., Rivalta, E., 2011. A quantitative study of the mechanisms governing dike propagation, dike arrest and sill formation. *Journal of Volcanology and Geothermal Research* 208, 39–50.
- Macdonald, K.C., 1982. Mid-ocean ridges: fine scale tectonic, volcanic and hydrothermal processes within the plate boundary zone. *Annual Review of Earth and Planetary Sciences* 10, 155–190.
- Machado, F., 1974. The search for magmatic reservoirs. In: Civetta, L., Gasparini, P., Luongo, G., Rapolla, A. (Eds.), *Physical Volcanology*. Elsevier, Amsterdam, pp. 255–273.
- MacLeod, C.J., Yaouancq, G., 2000. A fossil melt lens in the Oman ophiolite: implications for magma chamber processes at fast spreading ridges. *Earth and Planetary Science Letters* 176, 357–373.
- Marsh, B.D., 1989. Magma chambers. *Annual Review of Earth and Planetary Sciences* 17, 439–474.
- Marsh, B.D., 2000. Magma chambers. In: Sigurdsson, H. (Ed.), *Encyclopedia of Volcanoes*. Academic Press, New York, pp. 191–206.
- Masterlark, T., 2007. Magma intrusion and deformation predictions: sensitivities to the Mogi assumptions. *Journal of Geophysical Research* 112. <http://dx.doi.org/10.1029/2006JB004860> (Article number B06419).
- McKenzie, D.P., 1984. The generation and compaction of partially molten rocks. *Journal of Petrology* 25, 713–765.
- McTigue, D.F., 1987. Elastic stress and deformation near a finite spherical magma body: resolution of the point source paradox. *Journal of Geophysical Research* 92, 12,931–12,940.
- Melan, E., 1932. Point force at internal point in a semi-infinite plate. *Zeitschrift für Angewandte Mathematik und Mechanik* 12, 343–346 (in German).
- Menand, T., 2008. The mechanics and dynamics of sills in layered elastic rocks and their implications for the growth of laccoliths and other igneous complexes. *Earth and Planetary Science Letters* 267, 93–99.
- Menand, T., 2011. Physical controls and depth of emplacement of igneous bodies: a review. *Tectonophysics* 500, 11–19.
- Menand, T., Daniels, K.A., Benghiat, P., 2010. Dyke propagation and sill formation in a compressive tectonic environment. *Journal of Geophysical Research* 115. <http://dx.doi.org/10.1029/2009JB006791> (Article No. B08201).
- Menand, T., de Saint-Blanquat, M., Annen, C. (Eds.), 2011. Emplacement of magma pulses and growth of magma bodies. *Tectonophysics* 500, 1–112.
- Milne-Thompson, L.M., 1996. *Theoretical hydrodynamics*, 5th ed. Dover, New York.
- Mindlin, R.D., 1936. Force at a point in the interior of a semi-infinite solid. *Physics* 7, 195–202.
- Mogi, K., 1958. Relations between eruptions of various volcanoes and the deformations of the ground surfaces around them. *Bulletin of the Earthquake Research Institute* 36, 99–134.
- Moran, S.C., Newhall, C., Roman, D.C., 2011. Failed magmatic eruptions: late-stage cessation of magma ascent. *Bulletin of Volcanology* 73, 115–122.
- Murase, T., McBirney, A.R., 1973. Properties of some common igneous rocks and their melts at high temperatures. *Geological Society of America Bulletin* 84, 3563–3592.
- Mutter, J.C., Carbotte, S.M., Su, W.S., Xu, L.Q., Buhl, P., Detrick, R.S., Kent, G.M., Orcutt, J.A., Harding, A.J., 1995. Seismic images of active magma systems beneath the East Pacific Rise between 17-degrees-05's and 17-degrees-35's. *Science* 268, 391–395.
- Myrvang, A., 2001. *Rock Mechanics*. Norway University of Technology (NTNU), Trondheim. (in Norwegian).
- O'Driscoll, B., Troll, V.R., Reavy, R.J., Turner, P., 2006. The Great Eucrite intrusion of Ardnamurchan, Scotland: reevaluating the ring-dike concept. *Geology* 34, 189–192.
- Parfitt, E.A., Wilson, L., 2008. *Fundamentals of Physical Volcanology*. Blackwell, Oxford.
- Pasquare, F., Tibaldi, A., 2007. Structure of a sheet-laccolith system revealing the interplay between tectonic and magma stresses at Stordalur Volcano, Iceland. *Journal of Volcanology and Geothermal Research* 161, 131–150.
- Petford, N., Kerr, R.C., Lister, J.R., 1993. Dike transport in granitoid magmas. *Geology* 21, 845–848.
- Petford, N., Cruden, A.R., McCaffrey, K.J.W., Vigneresse, J.L., 2000. Granite magma formation, transport and emplacement in the Earth's crust. *Nature* 408, 669–673.
- Petraske, K.A., Dennis, S.H., Shaw, R., 1978. Mechanics of emplacement of basic intrusions. *Tectonophysics* 46, 41–63.
- Pinel, V., Jaupart, C., 2003. Magma chamber behavior beneath a volcanic edifice. *Journal of Geophysical Research* 108 (Art. 2072, February 4).
- Poland, M., Hamburger, M., Newman, A., 2006. The changing shapes of active volcanoes: history, evolution, and future challenges for volcano geodesy. *Journal of Volcanology and Geothermal Research* 150, 1–13.
- Pollard, D.D., 1976. Form and stability of open hydraulic fractures in the earth's crust. *Geophysical Research Letters* 3, 513–516.
- Pollard, D.D., Johnson, A.M., 1973. Mechanics of growth of some laccolithic intrusions in the Henry Mountains, Utah, II. Bending and failure of overburden layers and sill formation. *Tectonophysics* 18, 311–354.
- Rivalta, E., Bottiner, M., Dahm, T., 2005. Buoyancy-driven fracture ascent: experiments in layered gelatine. *Journal of Volcanology and Geothermal Research* 144, 273–285.
- Roobol, M.J., 1974. Geology of the Vesturhorn intrusion, SE Iceland. *Geological Magazine* 111, 273–285.
- Rosi, M., Papale, P., Lupi, L., Stoppato, M., 2003. *Volcanoes: Buffalo Firefly Books*.
- Rubin, A.M., 1995. Propagation of magma-filled cracks. *Annual Review of Earth and Planetary Sciences* 23, 287–336.
- Ryan, M.P., 1993. Neutral buoyancy and the structure of mid-ocean ridge magma reservoirs. *Journal of Geophysical Research* 98, 22,321–22,338.
- Saada, A.S., 2009. *Elasticity: Theory and Applications*. Krieger, Malabar, Florida.

- Satter, A., Ghulam, Iqbal, G.M., Buchwalter, J.L., 2008. Practical Enhanced Reservoir Engineering. PennWell, Tulsa.
- Saunders, S.J., 2001. The shallow plumbing system of Rabaul caldera: a partially intruded ring fault? *Bulletin of Volcanology* 63, 406–420.
- Savin, G.N., 1961. *Stress Concentration Around Holes*. Pergamon, New York.
- Schon, J.H., 2004. *Physical Properties of Rocks: Fundamentals and Principles of Petrophysics*. Elsevier, Oxford.
- Schultz, R.A., 1995. Limits on strength and deformation properties of jointed basaltic rock masses. *Rock Mechanics and Rock Engineering* 28, 1–15.
- Secor, D.T., Pollard, D.D., 1975. Stability of open hydraulic fractures in the earth's crust. *Geophysical Research Letters* 2, 510–513.
- Segall, P., 2010. *Earthquake and Volcano Deformation*. Princeton University Press, Princeton.
- Sibbett, B.S., 1988. Size, depth and related structures of intrusions under stratovolcanoes and associated geothermal systems. *Earth-Science Reviews* 25, 291–309.
- Siebert, L., Simkin, T., Kimberly, P., 2010. *Volcanoes of the World*, 3rd ed. University of California Press, London.
- Simkin, T., Siebert, L., 2000. Earth's volcanoes and eruptions: an overview. In: Sigurdsson, H. (Ed.), *Encyclopaedia of Volcanoes*. Academic Press, New York, pp. 249–261.
- Singh, S.C., Crawford, W.C., Carton, H., Seher, T., Combier, V., Cannat, M., Canales, J.P., Dusunur, D., Escartin, J., Miranda, J.W., 2006. Discovery of a magma chamber and faults beneath Mid-Atlantic Ridge hydrothermal field. *Nature* 442, 1029–1032.
- Sinton, J.M., Detrick, R.S., 1992. Mid-ocean magma chambers. *Journal of Geophysical Research* 97, 197–216.
- Sneddon, I.N., Lowengrub, M., 1969. *Crack Problems in the Classical Theory of Elasticity*. Wiley, New York.
- Sparks, R.S.J., Huppert, H.E., Turner, J.S., 1984. The fluid-dynamics of evolving magma chambers. *Philosophical Transactions of the Royal Society of London A* 310, 511–534.
- Spence, D.A., Sharp, P.W., Turcotte, D.L., 1987. Buoyancy-driven crack-propagation—a mechanism for magma migration. *Journal of Fluid Mechanics* 174, 135–153.
- Spera, F.J., 2000. Physical properties of magmas. In: Sigurdsson, H. (Ed.), *Encyclopedia of Volcanoes*. Academic Press, New York, pp. 171–190.
- Spera, F.J., Bohron, W.A., 2001. Energy-constrained open-system magmatic processes I: general model and energy-constrained assimilation and fractional crystallization (EC-AFC) formulation. *Journal of Petrology* 42, 999–1018.
- Stasiuk, M.V., Jaupart, C., Sparks, R.S.J., 1993. On the variation of flow rate in non-explosive lava eruptions. *Earth and Planetary Science Letters* 114, 505–516.
- Sturkell, E., Einarsson, P., Sigmundsson, F., Geirsson, H., Ólafsson, H., Pedersen, R., De Zeeuw-van Dalzen, E., Linde, A.T., Sacks, I.S., Stefánsson, R., 2006. Volcano geodesy and magma dynamics in Iceland. *Journal of Volcanology and Geothermal Research* 150, 14–34.
- Sun, R.J., 1969. Theoretical size of hydraulically induced horizontal fractures and corresponding surface uplift in an idealized medium. *Journal of Geophysical Research* 74, 5995–6011.
- Tada, H., Paris, P.C., Irwin, G.R., 2000. *The Stress Analysis of Cracks Handbook*. Del Research Corporation, Hellertown, PA.
- Taisne, B., Tait, S., Jaupart, C., 2011. Conditions for the arrest of vertical propagating dyke. *Bulletin of Volcanology* 73, 191–204.
- Tait, S., Jaupart, C., 1989. Pressure, gas content and eruption periodicity of a shallow, crystallizing magma chamber. *Earth and Planetary Science Letters* 92, 107–123.
- Tan, S.C., 1994. *Stress Concentrations in Laminated Composites*. Technomic, Basel.
- Thorarinnsson, S.B., Tegner, C., 2009. Magma chamber processes in central volcanic systems of Iceland: constraints from layered gabbro of the Austurhorn intrusive complex. *Contributions to Mineralogy and Petrology* 158, 223–244.
- Thordarson, T., Larsen, G., 2007. Volcanism in Iceland in historical time: volcano types, eruption styles and eruptive history. *Journal of Geodynamics* 43, 118–152.
- Thordarson, T., Self, S., 1993. The Laki (Skaftar Fires) and Grimsvotn eruptions in 1783–1785. *Bulletin of Volcanology* 55, 233–263.
- Trasatti, E., Giunchi, C., Bonafede, M., 2005. Structural and rheological constraints on source depth and overpressure estimates at Campi Flegrei Caldera, Italy. *Journal of Volcanology and Geothermal Research* 144, 105–118.
- Trasatti, E., Bonafede, M., Ferrari, C., Giunchi, C., Berrion, G., 2011. On deformation sources in volcanic areas: modeling the Campi Flegrei (Italy) 1982–84 unrest. *Earth and Planetary Science Letters* 306, 175–185.
- Valko, P., Economides, M., 1995. *Hydraulic Fracture Mechanics*. Wiley, New York.
- Wadge, G., 1981. The variation of magma discharge during basaltic eruptions. *Journal of Volcanology and Geothermal Research* 11, 139–168.
- Walker, B.A., Miller, C.F., Claiborne, L.L., Wooden, J.L., Miller, J.S., 2007. Geology and geochronology of the Spirit Mountain batholith, southern Nevada: implications for timescales and physical processes of batholith construction. *Journal of Volcanology and Geothermal Research* 167, 239–262.
- Wang, H.F., 2000. *Theory of Linear Poroelasticity*. Princeton University Press, Princeton.
- Warpinski, N.R., 1985. Measurement of width and pressure in a propagating hydraulic fracture. *Society of Petroleum Engineers Journal* 25, 46–54.
- West, M., Menke, W., Tolstoy, M., Webb, S., Sohn, R., 2001. Magma storage beneath axial volcano on the Juan de Fuca mid-ocean ridge. *Nature* 413, 833–836.
- Williams, J.G., 1980. *Stress Analysis of Polymers*, 2nd ed. Wiley, New York.
- Wilson, L., Head, J.W., 1981. Ascent and eruption of basaltic magma on the earth and moon. *Journal of Geophysical Research* 86, 2971–3001.
- Woods, A.W., Huppert, H.E., 2003. On magma chamber evolution during slow effusive eruptions. *Journal of Geophysical Research* 108 (B8), 2403. <http://dx.doi.org/10.1029/2002JB002019>.
- Yew, C.H., 1997. *Mechanics of Hydraulic Fracturing*. Gulf Publishing, Houston.
- Yu, H.-S., 2000. *Cavity Expansion Methods in Geomechanics*. Kluwer, London.
- Zang, A., Stephansson, O., 2010. *Stress Fields of the Earth's Crust*. Springer, Berlin.
- Zoback, M.D., 2007. *Reservoir Geomechanics*. Cambridge University Press, Cambridge.